NTNU

Norwegian University of
Science and Technology

High Temperature Cathodic Disbondin of Organic Coatings on Submerged Steel Structures

Håkon A Holm Gundersen

Chemical Engineering and Biotechnology
Submission date: June 2011
Supervisor: Kemal Nisancioglu, IMTE
Co-supervisor: Ole Øystein Knudsen, Sintef

Norwegian University of Science and Technology
Department of Materials Science and Engineering

Master Thesis, Spring 2011

High Temperature Cathodic Disbonding of Organic Coatings on Submerged Steel Structures

Norwegian University of Science and Technology

Department of Materials Science and Engineering

Håkon Gundersen

June 30, 2011

Supervisors:

Prof. Dr. Ole Øystein Knudsen
Prof. Dr. Kemal Nisancioglu

NTNU – Trondheim
Norwegian University of
Science and Technology

Abstract

There are currently no standard test methods for testing the cathodic disbonding properties of organic coatings at temperatures above 100 °C. There are several subsea oil and gas reservoirs with high temperatures, some as high as 200 °C. The main goal of this work was the development of a new apparatus and testing procedure for high temperature cathodic disbonding, hereby referred to as HTCD (High Temperature Cathodic Disbonding).

A test method for the cathodic disbonding of organic coatings from submerged steel subjected to high temperatures was studied. The test method requires the use of a specialized HTCD apparatus. In this test method, sample plates were mounted between two channels, one containing a hot (150 °C) oil flow and the other containing a pressurized, cold, salt (3.5 % NaCl) water flow. Accelerated conditions made it possible to test the cathodic disbonding properties of several coatings in four weeks. Four weeks is a typical duration for coating prequalification tests. Several commercial coating products of different generic types provided by different manufacturers were tested. The results indicate that adequate coating products for high temperature underwater exposure are available.

The required cathodic protection current for the samples tested in the HTCD apparatus was continuously monitored. No correlation between the required cathodic protection current and the extent of cathodic disbonding was observed.

A long term test with more field like conditions and a duration of 400 days was performed. Low levels of disbonding for most of the tested products in the 400 day test made comparison to the accelerated tests difficult.

An attempt was made to determine the oxygen diffusion coefficient of five coating products. The attempt was unsuccessful. The same method had previously been used to study coatings with a thickness of up to 300 µm, the coatings studied in this work were between 600 µm and 1200 µm. It remains uncertain whether the chosen method can be used for coatings this thick.

Results from electrochemical impedance spectroscopy, performed in a pressurized vessel, showed a large reduction in the ionic resistance of a submerged organic coating upon heating from 30 °C to 150 °C. This showed that elevated temperatures throughout the coating can reduce the ionic resistance to a level where even an intact coating is incapable of protecting the substrate. Studies of coating samples at ambient temperatures after exposure to higher temperatures showed that exposure to heat causes a lasting reduction in impedance. High impedances correlated with good performance in the HTCD tests.

Investigation with a scanning electron microscope (SEM) provided images where the extent of the cathodic disbonding was clearly visible. Electron-dispersive X-ray spectroscopy (EDS) enabled the identification of oxides discovered at the holiday and beneath the disbonded coating. Zinc and calcium oxides were identified at and near the holiday; iron oxide was identified beneath the disbonded coating.

Preface

This work was performed at the Norwegian University of Science and Technology (NTNU) in Trondheim, Norway. The work completes the course TMT4900, 'Materials Chemistry and Energy Technology, Master Thesis'. The work was done in cooperation with SINTEF Materialer og Kjemi and formed a part of a bigger project called 'High Temperature Cathodic Disbonding'. Parts of this thesis was based on the work performed in the projectreport from the course TMT4500, 'Materials Technology, Specialization Project'; all sections based on that work have been carefully reworked and updated.

I would like to thank my supervisors, Prof. Dr. Ole Øystein Knudsen at SINTEF and Prof. Dr. Kemal Nisancioglu of the Department of Material Science and Engineering at the Norwegian University of Science and Engineering (NTNU).

I would also like to thank Ann-Kristin Kvernbråten and Dr. Ole Edvard Kongstein. Special thanks go to Nils Inge Nilsen for valuable assistance with numerous practical problems.

Declaration

I declare that this work has been performed independently and in accordance with the rules and regulations at the Norwegian University of Science and Technology (NTNU).

Trondheim, June 30, 2011

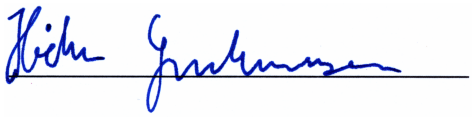

Håkon Gundersen

Contents

List of Figures

List of Tables

1 Introduction

Subsea structures are commonly made of carbon steel and require corrosion protection. Anticorrosive coatings are often used in combination with cathodic protection to preserve steel structures from corrosion.[1] Cathodic protection will in many situations be sufficient, but the addition of a good coating system can greatly reduce the current demand and therefore the required anode weight. A combination of a coating system and cathodic protection will often provide lower overall costs for a specified lifetime.[2]

The Kristin field is currently the hottest field on the Norwegian continental shelf, with a design temperature of 170°C. Even warmer fields have been developed in other parts of the north sea (Elgin-Franklin, 190°C). The Victoria field, currently planned for development, will be warmer still at 200°C. High temperatures in oil and gas reservoirs will in turn expose subsea steel structures to high temperatures. Coating these structures will present demands on the coating products that are quite different from those posed at milder temperatures.

During the lifetime of a subsea structure the coating system will start to degrade. As the coating system breaks down, the required protection current for the cathodic protection system will increase. Predicting and preventing coating degradation is therefore important in achieving the best possible performance. There are several mechanisms of coating degradation and cathodic disbonding is one of the most important.

Testing for cathodic disbonding is done according to internationally approved standards. There are currently no standardized tests for temperatures over 100°C, though there are some for warm conditions below 100°C. This leaves a substantial gap to the 200°C reservoir temperatures in the warmest oil and gas fields. It is clear that prequalification of the coatings used on these fields will require new test methods.

The purpose of this and previous work was to document a new, reliable test method for the cathodic disbonding behavior of different coating systems at high temperatures. This work is a continuation of my specialization project from the fall of 2010.[3] Several commercial coating products were subjected to extensive testing in terms of high temperature cathodic disbonding performance. The results from the accelerating cathodic disbonding tests were compared to those of a long term test performed at near-field conditions.

The proposed test method exposed samples to an environment of relatively cool saltwater environment while the backs of the samples were heated by 150 °C oil. The saltwater was pressurized to avoid boiling. Tests of different durations up to 28 days were performed. A 28 day duration has become the industry standard for prequalifying coating products. A high temperature test with a duration of 28 days could be compared to low temperature tests of the same duration.

Impedance measurements were made to supplement the disbonding tests. The impedance of a coating system is a measure of the coating's resistance to ion

transport. An attempt was made to determine the coefficient of diffusion of oxygen in the coating products. The transport of ions and oxygen through the coating are determining factors for the durability of a coating.

Additionally a disbonded coating was studied in the scanning electron microscope (SEM) to confirm that the results of the disbonding process can be identified in a cross section. Electron-dispersive X-ray spectroscopy (EDS) was used to identify oxide species near the holiday and at the coating-substrate interface.

2 Theory

This section gives an introduction to organic anticorrosive coatings, their protective mechanism, mechanism of adhesion and barrier properties. Special attention is given to the coating degradation mechanism known as cathodic disbonding. An introduction is also given to heat transport through a submerged coating, and the analytical methods of impedance spectroscopy and scanning electron microscopy (SEM).

2.1 Anticorrosive Coatings

Organic coatings are used for a multitude of purposes, including corrosion protection, decoration, texture, insulation and anti-fouling.[4] Further discussion will be limited to marine anti-corrosive coatings. Anticorrosive coatings are commonly applied to subsea structures in combination with cathodic protection. A good anticorrosive coating will reduce the current demand for the cathodic protection and thereby decrease the required anode weight, thus decreasing the total weight and cost of the cathodic protection system.[2]

Anticorrosive coatings usually consist of multiple layers of different coatings with different properties.[1] Some standards require these layers to be of contrasting colours.[5] The substrate is typically first covered with a primer, then one or more intermediate coats and finally a top coat.[1] The main purpose of the primer is to provide good adhesion between the substrate and the coating system. In addition to providing a sound base for the coating system, primers also provide corrosion protection.[1][6] The intermediate coat(s), sometimes called 'undercoat'[6], is applied on top of the primer and add to the barrier properties of the coating system, thus impeding the transport of agressive species.[1] The top coat is the final layer of the coating system and protects the coats beneath from the environment, adds to the corrosion protection properties and gives the system the desired colour.[6] Environmental degradation can come from temperature variation, ultraviolet (UV) radiation, moisture and impact.[1] The whole coating system contributes to the resistance against most of these factors, but UV radiation is blocked by the top coat. The top coat should be resistant to all of these factors, espescially UV radiation. Resistance to UV radiation is not necessary for primers and intermediate coats.

Studies of commercial coating systems remain relatively rare, as most papers regard 'model' systems, most often consisting of one organic film on a metal substrate.[7] Six commercial coating systems were investigated in this study, all of which have a thickness of over 500 µm, well beyond the range usually considered 'thick' for a model system. This should be kept in mind when comparisons are made to previous studies, as thinner, less complex, coating systems might display certain characterstics more distinctively than thick commercial coatings.

2.1.1 The Basic Constituents of Organic Coatings

Organic coatings usually consist of binders, pigments, solvents, fillers (extenders) and other additives.[1][2] The additives can include wetting agents, drying agents, corrosion inhibitors, thickeners and more.[1][2] Different coatings are created by changing the types and amounts of these constituents.

Binders provide the basic physical and chemical properties of the coating.[8] The mechanism of the film formation, the transition from a liquid product to a solid coating, is determined by the type of binder. The film can be formed through the evaporation of solvents (physical drying), through chemical reactions (chemical curing) or through a combination of the two.[1]. Physically drying and chemically curing coatings are further divided into subcategories based on what type of binder is used. Commonly used binders for physically drying coatings include chlorinated rubbers, vinyl chlorides, acrylics and polyurethane dispersions.[6] Commonly used binders for chemically curing coatings include epoxies (polyepoxide) and modified epoxies (modified with hydrocarbons, coal tar, etc.), polyurethanes, alkyl- and ethyl silicates.[6] Only coatings with different epoxy binders were used in this work.

Pigments are solids that are added to coatings to improve certain properties. Pigments can provide colour or opacity, improve barrier properties, provide corrosion protection and can improve the mechanical properties of a coating.[1][8] For anti-corrosive coatings the barrier properties and corrosion protection are the most interesting aspects. Barrier properties are improved by any pigment that is impermeable to aggressive species.[1] Flake shaped pigments are used to specifically improve barrier properties.[1][2] Glass flakes, aluminium flakes, titanium dioxide and micaceous iron oxide are examples of flake shaped pigments. Flake shaped pigments have a tendency to orient themselves paralell to the substrate and greatly increase the diffusion paths of aggressive species.[1][2] Too high concentrations of pigments can reduce the effectiveness of a coating.[9] Significant changes occur at the critical pigment volume concentration,[9] above which not all of the solid particles are covered with polymer and not all the gaps between the particles are filled with polymer. Zinc silicate coatings are often pigmented above the critical pigment volume concentration.[1]

Some pigments provide active corrosion protection, either through sacrifice or inhibition. The most common sacrificial pigment is zinc. Zinc particles are preferentially sacrificed to provide galvanic protection to the substrate.[10] A relatively high zinc pigment content is necessary to achieve the necessary electrical contact.[1] Other pigments form complexes with certain aggressive ions such as chloride or form a protective oxide film on the substrate. Zinc phosphate is a common 'green' pigment, used as a replacement for toxic chromate pigments.[11][12] Aluminium pigments, in addition to contributing to the barrier effect, may lower the pH at the coating-substrate interface. The effect of aluminium particles on cathodic disbonding will be discussed in further detail in section 2.2.

Solvents are added to coatings to dissolve or disperse the other constituents.[1] Solvents change the rheology of the coating and is important for application and film formation purposes. Organic liquids that evaporate at the prevailing temperatures

and atmospheric pressure are termed volatile organic compounds, or VOCs.[6] Most organic solvents are classifieds as VOCs. There are several problems assosciated with VOCs, including human health risks, fire- and explosion hazards.[1] The risks have resulted in legislation limiting the use of VOCs in the coating industry. There are several alternatives to solvent-borne coatings, including powder coatings, solvent-free coatings and waterborne coatings.[1]

Fillers, or extenders, are inorganic solids that are added to coatings to reduce costs. Fillers usually do not improve the anticorrosive characteristics of a coating significantly, though some fillers have been shown to improve certain properties.[1]

Other additives are included to improve certain properties (e.g. wetting) or solve certain problems (e.g. foam formation).[1]

2.1.2 Protective Mechanism

There are several relevant protective mechanisms for organic coatings. The relative importance of each depend on both the coating system, the environment and the substrate. Coatings can act as a barrier against the diffusion of ions, water and oxygen. Coatings can prevent the formation of an aqeous phase at the coating-substrate interface. Coatings cause an extension of the electrical double layer, thus reducing the corresponding electrical field strength. Finally coatings may act as vehicles for anticorrosive pigments, as was discussed in section 2.1.1.[8][10][13]

Corrosion is an electrochemical process, thus an electrolyte and an oxydizing species must both be present at the metal surface for corrosion to occur.[13] For coated systems the coating-metal interface is considered, rather than a bare metal surface. In most practical examples corrosion will require the transport of water, oxygen and ions through the coating to the coating-metal interface.[13] Oxygen and water are consumed in the resulting corrosion reaction, combining with iron to form hydrated iron oxides or iron oxide hydroxides (i.e. rust), an example is shown in equation 2.1 where lepidocrocite is formed.[10] The rate determining factors for the corrosion can therefore be the transport of water, oxygen or the electrochemical reaction itself.[13]

$$4Fe + 3O_2 + H_2O \rightarrow 4FeOOH \tag{2.1}$$

The electrochemical reaction presented in equation 2.1 is the sum of two half-reactions, one anodic and one cathodic. In this case the anodic half-reaction was the oxidation of iron, whereas the cathodic half-reaction was the reduction of oxygen. For systems with cathodic protection, the cathodic reaction is frequently the only reaction that occurs at the coating-metal interface, while the anodic reaction occurs at a sacrificial anode. Two possible half-reactions for the reduction of oxygen and water are presented in equations 2.2 and 2.3.[2]

$$2H_2O + 2e^- \rightarrow H_2 + 2OH^- \tag{2.2}$$

$$O_2 + 2H_2O + 4e^- \rightarrow 4OH^- \tag{2.3}$$

Organic coatings present imperfect barriers against the transport of water and oxygen. Coatings act as a barrier against diffusion, pigmentation with flake-shaped pigments espescially increases the barrier effect against oxygen diffusion.[2] The average concentration of both oxygen and water in a coating is nevertheless several times higher than the concentration necessary to initiate corrosion. In other words, the supply of water and oxygen at the coating-substrate interface is sufficient to cause corrosion. Hence coatings do not protect the substrate by blocking the transport of water and oxygen, though the barrier effect may contribute to the overall protective mechanism.[10][13] It should be noted that highly polar polymers often are excellent oxygen barriers, but poor water barriers, whereas the opposite is true for highly non-polar polymers.[14]

Organic coatings are efficient barriers against the transport of ions. Due to their charged nature, the transport of ions is inherently more complex than that of water or oxygen.[2] The transport of ions rely on electric fields, other charged species, polar groups and water. Transport of ions through organic coatings has previously been explained by the formation of conductive pathways[15] and by preceeding water uptake[16]. It has been suggested that the two mechanisms need not be mutually exclusive if the creation of conductive pathways is a consequence of water uptake.[17] Cracks and crevices resulting from mechanical, thermal or residual stresses following the coating's application can act as conductive pathways when filled with electrolyte.[2][17]

An increase in ion concentration can either increase or decrease the ionic conductivity in a coating.[2][16][17] Such an increase in conductivity is referred to as 'direct' or D-conductivty, while a decrease in conductivity is referred to as 'indirect' or I-conductivity. Areas with D-conductivity will absorb more water and have a significantly lower ionic resistance than areas with I-conductivity.[17] Coatings with cross-linked binders will typically display a mixture of areas with I-conductivity and areas with D-conductivity, non-cross-linked coatings will only display D-conductivity.[2][16] The occurence of both types of conductivity in a coating is caused by inhomogeneous levels of cross-linking of the binder in different areas. Areas with a high degree of cross-linking will show I-conductivity, while areas with little cross-linking will show D-conductivity. Highly cross-linked areas will only absorb water, not ions. The conductivity in the coating will therefore depend on the activity of water in the solution. Areas with little cross-linking will be permeable to ions, thus the conductivity in these areas will depend on the conductivity in the electrolyte.[2] Thicker coating films and multiple coats decrease the number of areas with D-conductivity.[2]

The main protective mechanism of organic coatings is in the effective prevention of electrochemical reactions. The driving force of electrochemical reactions is an electric field. Normally a submerged metal will be surrounded by an electric double layer, a region of adsorbed ions. The larger and less hydrated anions are more strongly adsorbed to the metal than cations, which leads to a negative charge on the immideate metal surface. There is a higher concentration of hydrated cations

in the solution close to the surface, which ensures the local charge balance. In total this provides a charge difference over a distance which is only a few molecular layers thick, which results in a very strong electric field.[4] When a coating with a sufficient ionic resistance is present on the metal surface the electric double layer is extended over a much larger distance, the thickness of the coating, hence the electric field strength is reduced. With a reduced electric field strength the driving force for electron-transfer is reduced and any electrochemical reaction involving the metal is hampered.[1][8][13]

A barrier coating will only be successful in protecting the substrate as long there is no water phase present at the coating-substrate interface. The penetration through the coating and accumulation beneath the coating of ions will lead to an osmotic pressure across the coating. Thus, penetration by ions will lead to the creation of a water phase beneath the coating.[1] The creation of a separate aqueous phase beneath the coating will greatly increase the charge transfer kinetics. This can lead to the failure of intact coatings.[13][17]

2.1.3 Oxygen Diffusion

Oxygen is a small, non-polar molecule and the concentration of oxygen in a submerged organic coating is lower than that of water. The result is that oxygen diffusion in organic coatings is closer to ideal, in the sense that Fick's and Henry's laws apply to a larger degree than for water.[2] Studies have shown that the oxygen concentration throughout a typical anticorrosive coating is large enough to allow corrosion or disbonding reactions.[1][13]

The permeation of a gas through a polymer film is thought to involve several stages: absorption into the polymer, solubilisation in the polymer matrix and diffusion through the polymer down a concentration gradient. Of these, solubilisation and diffusion are possible rate-determining steps.[14] For the transport of oxygen through an organic coating, the diffusivity is usually the dominating term.[14]

Oxygen diffusion has been measured in freestanding films[14], with the reference electrode placed under the coating[13] and on coated sample panels.[2] These diffusion experiments utilize the delay-time method[18] which allows the determination of both diffusion coefficient and permeability.

2.1.4 Adhesion

The protective qualities of organic coatings greatly depend on their ability to adhere to the substrate[1][4], some go as far as calling it 'the most important and decisive property'[19]. In contrast to this, some studies have shown that the properties of adhesion and corrosion resistance need not correlate in all cases.[20][21]

Adhesion is the result of physical and chemical forces. A number of different forces and bonds can be the basis of adhesion. The possible types are mechanical bonds, chemical bonds, intermolecular forces and electrostatic forces.[2] The elec-

Table 2.1: Binding Energies relevant to Adhesion[22]

Type of Force	**Energy Range** [kcal/mol]
Chemical Bonds	
Ionic	140-250
Covalent	15-170
Metallic	27-83
Intermolecular Forces	
Hydrogen bonds	up to 12
Dipole–dipole	up to 5
Dipole–induced dipole	up to 10
Induced dipole–induced dipole	up to 0.5

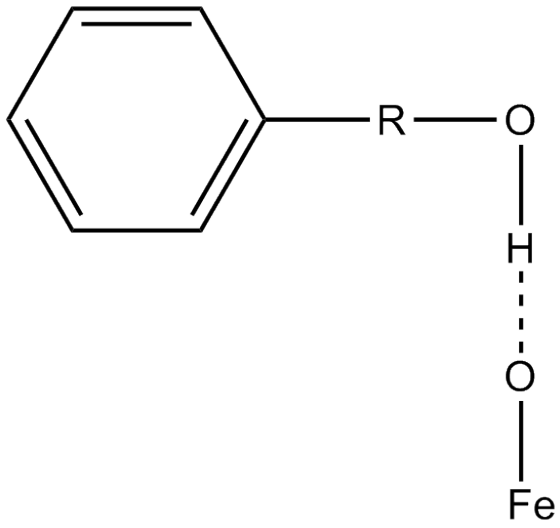

Figure 2.1: Adhesion of epoxy to the ferrous oxide layer on steel by hydrogen bonds. Adapted from [1]

trostatic forces and mechanical bonds provide minor or insignificant contributions to adhesion[2][19]. Chemical bonds are strong, but whether or not they exist as adhesive bonds is unclear. If chemical bonds occur between a coating and the substrate their contribution to adhesion would be significant[2]. Intermolecular or van der Waals forces are distinguished into three types: forces between two permanent dipoles (Keesom), forces between a permanent dipole and an induced dipole (Debye) and forces between two induced dipoles (London dispersion force). Hydrogen bonds are a special case for compounds with covalently bonded hydrogen. It is generally believed that most organic coatings adhere to metals via intermolecular forces, specifically hydrogen bonds.[1] This is shown in figure 2.1. Table 2.1 provides an overview of the energy involved in the different types of forces that may contribute to adhesion. In addition to these, interdiffusion and polymer entanglement are mechanisms that may contribute greatly to cohesion/autohesion, but probably not to substrate-coating adhesion.[1][20]

2.1.5 Pre-Treatment

The cleanliness and roughness of the substrate are both important for the adhesion of a coating.[1] Up to a certain point an increase in surface roughness provides an increase in adhesion. This increase has been explained by an increase in surface area, increased reactivity of the substrate and the formation of mechanical bonds.[1] The contribution from mechanical bonds is likely minor, except for porous substrates, though the effect of lateral forces have not been studied extensively.[2] The presence of grease, dirt, oxides, old coatings or other matter on the substrate surface can significantly reduce adhesion.[1] This hampers adhesion by the simple mechanism that any coating applied on top will bond to these contaminants instead of to the substrate itself. The adhesion of the coating is then limited by the adhesion of the dirt or grease to the susbtrate, which is generally poor.

The presence of contaminants and the surface topography can both be controlled, to some extent, by applying the correct pre-treatment.[23] Grit-blasting can remove contaminants, including old coatings, and increase surface roughness.[20] Water-blasting can remove other contaminants, ultra-high-pressure water-blasting can remove old coatings, but does not affect the surface roughness. A substrate contaminated with ions may provide sufficient adhesion immidiately following the application of a coating, but the ions may subsequently lead to an osmotic pressure build up and blistering, as discussed in section 2.1.2. The importance of the correct pre-treatment should be stressed, an estimated 70% of all coating failures are caused by poor or inadequate surface preparation.[10]

Special pre-treatment processes may increase the adhesion or corrosion resistance of a coating system. The relative effects of processes like, chromating, phosphating, silanisation and thin electropolymer films on adhesion and corrosion performance have been studied.[20][21] These processes have seen extensive applications in the coatings industry, but the details of their mechanisms and effects are beyond the scope of this thesis.

2.1.6 Coating Degradation

Coatings are complex systems involving numerous components; they are exposed to diverse environments and thus the different modes of coating degradation and failure are equally numerous. The modes of failure can generally be divided into those that cause cosmetic defects, and those that cause corrosion.[1] The causes of failure are generally divided into those related to improper pre-treatment or application and those caused by environmental exposure.[10] Cosmetic degradation include colour fading, loss of gloss and chalking. Most cosmetic degradation of organic coatings on steel is caused by a degradation of the binder after exposure to UV-radiation.[1] Degradation that leads to corrosion includes blistering, erosion, peeling/flaking, corrosion creep and cathodic disbonding.[1][10] The discussion of all of these degradation mechanisms is beyond the scope of this thesis, but the mechanism of cathodic disbonding is given special attention in section 2.2. It should be noted that many parameters are important with regards to the lifetime and

breakdown of an organic coating system. These parameters include pre-treatment, paint formulation, pigments, environmental exposure, mechanically induced damage (scratches and holes), paint application and more. Since many parameters are important, the system, as a whole, should be considered when the performance of organic coatings is discussed.[10]

Norsok M503[24] operates with a coating breakdown factor f_c, which corresponds to the ratio of the necessary cathodic protection current density for a coated and an uncoated sample, i.e. $f_c = \frac{i_{coated}}{i_{uncoated}}$. The coating breakdown factor thus summarizes the complete state of a coating, with regards to corrosion protection, in a single number. In addition to providing a tool for calculating the necessary anode weight for systems protected by a combination of coatings and cathodic protection, the breakdown factor suggests that the extent of coating breakdown can be observed by measuring the current demand for cathodic protection over time. However, Knudsen and Steinsmo[25] found that cathodic disbonding from a coating holiday will not significantly increase the current demand for cathodic protection. Previous studies of the same coating products used in this work did not reveal any correlation between the current demand for cathodic protection and the extent of cathodic disbonding.[3]

2.2 Cathodic Disbonding

Cathodic protection and organic coatings are often combined to protect submerged steel structures. An organic coating system reduces the necessary protection current for the cathodic protection. Likewise, the combination provides protection to any areas where the coating system is damaged compared to just using a coating.[1] Cathodic disbonding is a degradation process that causes a loss of adhesion between a coating and the substrate. This disbonding often occurs for substrates that are protected by both cathodic protection and a coating system. Cathodic disbonding can also occur without cathodic protection when the separation of cathodic and anodic sites beneath the coating leads to the same local driving force.[10][26] Various terms including cathodic disbondment, cathodic delamination and cathodic adhesion loss are used, in litterature, as a term for the same mechanism.

2.2.1 Mechanism

Cathodic disbonding is a degradation process that causes a loss of adhesion between a coating and the substrate. The loss of adhesion occurs on cathodic areas of the substrate.[2] There the cathodic reaction (equation 2.2 or 2.3 in section 2.1.2) will create a high pH environment which will disrupt the adhesion of the coating and passivate the steel. The result is a loss of adhesion without subsequent corrosion of the substrate.

The mechanism of cathodic disbonding is illustrated in figure 2.2. The disbonding is initiated at a damaged area of the coating where the substrate is exposed to the electrolyte (a holiday). The cathodic reaction (Equation 2.3) is limited to sites where the substrate is exposed, at the holiday and under the coating around the holiday.

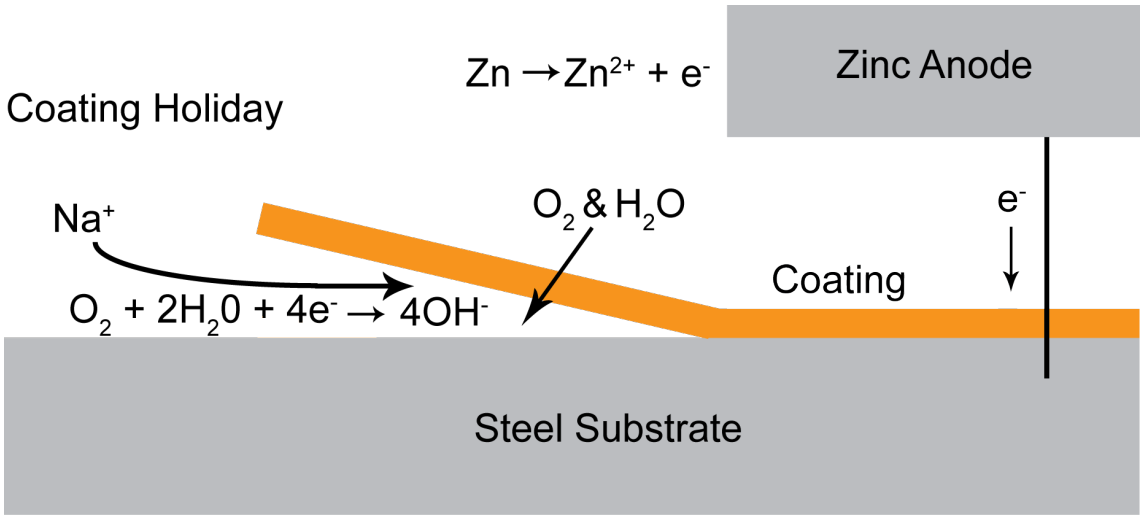

Figure 2.2: Cathodic Disbonding

Oxygen reduction is the dominating reaction at the disbonding front. The anodic reaction will occur at the anode, which is spatially separated from the cathodic area. The substrate is protected by a zinc anode in figure 2.2. The reaction product of the cathodic reaction will raise the pH of the environment in the holiday to the point where the adhesion between the coating and the substrate is lost. A pH value as high as 12 to 14 has been observed.[1] When the adhesion is lost a larger area of the substrate is exposed to the electrolyte and the disbonding propagates beneath the coating film, during this propagation the oxygen and water needed for the reaction diffuses through the disbonded coating film. Charge balance beneath the disbonded coating is maintained by the diffusion of cations through the electrolyte beneath the coating.[1][26] The diffusion of cations is believed to be the rate-determining step[1] and linear propagation correlating with Fickian diffusion control has been observed.[1][26]

Recent investigation indicates that free radicals can be involved in the cathodic disbonding mechanism. The inclusion of free radical scavengers in coating formulations resulted in a reduction of the rate of cathodic disbonding of up to 50%.[27] Cathodic polarization allows for the reduction of oxygen to reactive intermediates, examples are given in equations 2.4 and 2.5. Free radicals may explain the increase in rate of cathodic disbonding for systems with an externaly applied cathodic protection. Free radicals were suspected after chemical compounds that could only be the result of highly reactive intermediates were observed in several types of coatings after delamination.[27]

$$\frac{1}{2}O_2 + H_2O + e^- \rightarrow \cdot OH + OH^- \tag{2.4}$$

$$O_2 + e^- \rightarrow \cdot O_2^- \tag{2.5}$$

2.2.2 Testing for Cathodic Disbonding

There are several standardized methods for testing the resistance of a coating system against cathodic disbonding, including ISO 15711[28], ASTM G8[29], ASTM G42[30] and ASTM G95[31]. All of these tests are accellerated and utilize artificial holidays and environments that are more hostile to the coating system than that likely encountered in the field. Of these ISO 15711 and ASTM G8 describe tests involving the submersion of test plates in an electrolyte bath and providing cathodic protection, either through impressed current by a potentiostat or by attached sacrificial anodes. ASTM G95 describes a test method where the test cell is attached to a larger test object. ASTM G42 provides a test method for testing at elevated temperatures ($\sim 60°C$) with an impressed current. None of these cover temperatures in the range considered by this project.

There have been some recent proposed methods of testing at elevated temperatures. The HTCD apparatus used in this work was first developed by Knudsen et al[32] and has previously been succesfully used to perform cathodic disbonding tests at elevated temperatures.[33][34] This apparatus fix sample plates between two channels. One of these channels carries a cooled electrolyte past the coated side of the sample plates. The other channel carries heated oil past the back side of the sample plates. Cathodic protection is provided by a potentiostat. The strength of this test is that the samples are subjected to the temperatures expected in field use while keeping the electrolyte at moderate temperature levels. More recently Al-Borno presented a method for testing cathodic disbonding at temperatures over 100°C in an autoclave[35]. Testing of cathodic disbonding in an autoclave has also been demonstrated by Melve and Ali[36]. Testing in autoclaves involves heating the electrolyte to the same temperature as the sample plates, which is unrealistic when compared to the conditions encountered in the field.

The difficulty of testing at temperatures above the normal boiling point of the electrolyte may be circumvented by raising the boiling point by adding large concentrations of easily soluble salts. The theory of this method was discussed by Shukla et al.[37] It is likely that changing the electrolyte chemistry drastically from that of sea water will affect the performance of the coatings.

The need for a separate, and complex, high temperature test for cathodic disbonding was investigated in my specialization project. Paralell testing of the same samples in the accelerated, high temperature test, a long term test at near-field conditions, a test performed in an autoclave and a standard room temperature test in accordance with ISO-15711 was performed. The accelerated test resulted in relative performance comparable to that of the near-field test. The ISO-15711 test did not correlate with any of the high temperature tests. Tests performed in an autoclave were shown to be more severe than, and correlate poorly with, the HTCD apparatus and the near-field test. From these results it was concluded that there is a need for a separate high temperature cathodic disbonding test, and furthermore that an autoclave test is not a good candidate.[3][33][34][38]

The disbonded area is assessed in much the same fashion for all the standard tests. The coating is cut with a sharp knife or scalpel, making one or more cuts through

the holiday. The knife or scalpel is then used in an attempt to lift or peel the coating back, any loss of adhesion is noted. The size of the area (if any) around the holiday where the coating suffered from reduced adhesion is noted. The exact number of, and position of, cuts prior to peeling/lifting differs between the standards.

Assessing the disbonded area for very thick and hard coatings can be difficult. Test results from samples of some of the same coating products used in this test were previously assessed with an alternate method.[3] In cases where the normal method proved inadequate, a sheath knife and a mallet were used to knock of the coating. Distinguishing the strength of adhesion with this method is difficult, but a discolored area on the substrate around the holiday was observed for many coating systems. This discolored area, a darkened ring, corresponded with the disbonded area for several samples tested in the usual manner. This discoloration may be a valid indicator of the extent of disbonding.

Recent efforts have been made to develop non-destructive methods of assessing the extent of disbonding. Scanning acoustic microscopy (SAM) has been used to characterize coatings with regards to disbonding, blistering and topology, and to study disbonding mechanisms.[39][40] The scanning Kelvin probe has seen much use in the study of cathodic disbonding. The technique allows measurement of the voltage between a substrate and the probe, even through highly insulating organic coatings. The ability to make independent measurements at defects and compare them with intact areas allows study of the rate of cathodic disbondment non-destructively.[1][8][41][42][43][44]

Results indicate that elevated substrate temperatures can accelerate the cathodic disbonding process.[3][32][33][34] Despite this, there is no special mention of elevated substrate temperatures in any of the standards used in Norwegian offshore. The poor correlation with room-temperature tests[3] illustrates the need for a pre-qualification test for coatings that are to be put to high temperature use.

2.2.3 Parameters for Cathodic Disbonding

A small litterature study of the effect of the relevant parameters on cathodic disbonding was performed as a part of my specialization project.[3] Knudsen reviewed the relevant litterature discussing the parameters for cathodic disbonding in 1998.[2] The study therefore focused on litterature published after 1998. The factors considered by Knudsen were oxygen concentration, electrolyte type and concentration, applied potential, dry film thickness, time dependence, pre-treatment and paint composition.

Oxygen Concentration: Knudsen identified from earlier litterature that no, or only insignificant, cathodic disbonding occurs in the absence of dissolved oxygen. In addition a decrease in oxygen concentration led to a decrease in cathodic disbonding.[2] Sørensen compared the behavior of a system with a constant supply of pure oxygen to a non-aerated system. The results indicate that increased oxygen concentration increases the rate of cathodic disbonding.[45] Sørensen proposed that the increased concentration of oxygen would affect the potential difference between

the anode and the cathode through the cathodic reaction (Equation 2.3). The potential gradient is a driving force for the transport of cations to the site of the cathodic disbonding. Disbonding behavior for oxygen-free atmospheres, as well as different partial pressures of oxygen were studied by Leng et al[43] the results correlate with a dependency of cathodic disbonding on oxygen concentration.

Electrolyte Type: Cathodic disbonding has been found to increase with cation type in the order: Ca^{2+}, Li^{+}, Na^{+}, K^{+},Rb^{+}, Cs^{+}.[2][42][46] This corresponds to the mobility of the ions in water.[2] Disbonding in solutions with divalent cations has been shown to be very low, this is likely due to the low solubility of the hydroxides of these cations.[2] Leng et al[42] found that although the rate of cathodic disbonding can be ranked in accordance with cation mobility, the difference in disbonding rate was larger than the difference in mobility would suggest. However, later studies have shown that the disbonded area and the mobility of the cation follow a linear relationship.[47]

Cathodic disbonding has been found in earlier litterature to be independent of the anion type.[2] Later studies suggest some minor changes in rate upon changes in anion type, but nevertheless conclude that anion type is not essential for the disbonding mechanism.[42]

Electrolyte Concentration: The rate of cathodic disbonding decreases with increased electrolyte concentration.[2] This can be due to changes in the activity of water and thus the concentration of water in the coating. Increased electrolyte concentration also affects the solubility of oxygen. Leng et al[42] found that no disbonding occurs for very dilute solutions. A minimum electrolyte concentration at the metal-coating interface is necessary to form the galvanic connection.

Applied Potential: There is a linear relationship between the applied potential of the cathodic protection and the rate of cathodic disbonding.[2][45] Sørensen et al. performed an experiment where the ionic transport was confined to the coating-steel interface by using a setup of double cylinders which enclosed the electrolyte to the coating holiday on a coated sample plate. This experiment did not show any corresponding relationship between the applied potential and the rate of cathodic disbonding. This indicates that increasing potentials accelerate disbonding by facilitating ionic transport through the coating.[45]

Dry Film Thickness Increased film thickness leads to decreased cathodic disbonding.[2] Zhou and Jeffers confirm this in a later study with testing temperatures as high as 65 °C.[48] Results in a recent study indicated that an epoxy coating system containing aluminium flakes can display a disbonding behavior independent of film thickness.[47] Aluminium pigments are discussed in more detail in the paragraph on paint composition.

Pre-Treatment Increased surface roughness has been shown to decrease cathodic disbonding. Increased contact area between substrate and coating, and increased diffusion path for cations along the coating-steel interface are proposed mechanisms.[2] The relationship between pre-treatment and adhesion in general was discussed in subsection 2.1.5. In a recent study the rate of disbonding was shown to depend on the tortuosity of the cation diffusion path.[23] Greater tortuosity can be achieved by abrasive cleaning, parameters that affect tortuosity include grain size and speed during grit blasting. Increased tortuosity alone did not prevent cathodic disbonding completely, but slowed the rate of disbonding.

Incorrect surface pre-treatment can lead to blistering, a different coating failure mechanism. This can make it difficult to evaluate the performance of a coating with regards to cathodic disbonding, since the conditions of a cathodic disbonding test can also promote blistering.

Paint Composition Early litterature on the effect of paint composition on cathodic disbonding is limited. One study showed that an epoxy-amine system performed better than an epoxy-ester and an epoxy urethane. Another study showed that aluminium pigments reduced cathodic disbonding.[2] Sørensen found a correlation between an increased amount of secondary hydroxyl-groups in the uncured epoxy and reduced disbonding. The effect of crosslinking and rigidity on disbonding was limited.[45]

Pigmentation increases the resistance against cathodic disbonding. It has been found that flake-shaped pigments are more effective than spherical pigments.[45] Flake-shaped pigments have been found to arrange themselves parallel to the substrate and are believed to increase the barrier properties of the coating.[2] Aluminium pigments have been found to be highly effective against cathodic disbonding. A buffer mechanism has been proposed. The environment at the disbonding front can reach pH levels as high as 14.[1] Aluminium is not stable in aqeous solutions above pH 9 -10. Results have shown that aluminium pigments in disbonded coatings corrode. The corrosion of aluminium pigments near the disbonding front would lower the pH there, thus inhibiting the disbonding mechanism.[2] The greater effect of aluminium pigments compared to other pigments has only been observed for pigments in the first coat, which strengthens the theory that aluminium react directly with the disbonding environment.[2]

Time Cathodic disbonding propagates in a linear fashion.[2][26] That is, the disbonded area is proportional to time, meaning that the disbonded radius is proportional to the square root of time. After the start of an experiment it is often found that a certain initiation period, where no disbonding is observed, precedes the linear propagation of disbonding. Leidheiser refers to this as 'delay time' and attributes it to the ingress of water, oxygen and ions into the coating.[26]

2.2.4 High Temperature Cathodic Disbonding

Previous results show that high temperatures increase the rate of cathodic disbonding.[3][32][33][34][36][35][46] The standard tests include methods for testing up to temperatures of 60 °C, but relevant temperatures in the field can go substantially higher (e.g. Kristing field 140 °C at wellhead[49]). Testing at temperatures above 80-90 °C is problematic, mainly due to electrolyte evaporation.[35] Room temperature tests correlate poorly with high temperature tests and cannot be used to prequalify coatings for high temperature service.[3][33] There is no constant correlation between coating performance at ambient and elevated temperatures.[3][33] In order to evaluate the performance of a coating at high temperatures, the coating must be tested at high temperatures.

2.3 Zinc as a reference electrode

Reference electrodes are essential components in electrochemical systems. A single potential cannot be measured, instead the potential difference between a reference electrode of known potential and the system one intends to study is measured. In order to fullfill their role, reference electrodes need to maintain a stable and known potential throughout the experiment.[50] Certain disadvantages are apparent with the conventional reference electrodes when pressurized or heated systems are to be studied. Liquid-filled Hg/Hg_2Cl_2 Cl^- (calomel) and $Ag/AgCl$ Cl^- electrodes are mechanically fragile and face limited suitability at high pressures and temperatures.[50]

Zinc has been used as a reference electrode in cathodic protection engineering.[51] The advantages of zinc electrodes include a stable potential, high exchange current, low resistivity, easy manufacture, low cost, long life and high strength.[51] The variation of the potential of zinc in salt water is small within the parameters expected in this work. The potential is stable with regards to salinity above about 0.15 M NaCl (approx. 9 g/l), with regards to temperature between 290 K and 310 K and fluctuations in oxygen concentration. The variations in potential were found to be less than ±10 mV.[51] The flow velocity of the electrode affected the potential of the zinc electrode, increased velocity moved the potential in the positive direction. An increase from 0 to 1.5 ms^{-1} moved the potential about 30 mV in the positive direction.[51]

2.4 Electrochemical Impedance Spectroscopy

Electrochemical impedance spectroscopy is an experimental method which has seen successfull use in several fields, including corrosion and coatings technology with regards to barrier properties[52], pigmentation[11] and cathodic disbonding[12].

2.4.1 General Introduction

The basis of impedance techniques is the perturbation of an electrochemical cell with an alternating signal. An example of such a perturbation is a sinusoidal variation in the applied voltage. Such a variation is expressed by equation 2.6, where V(t) is the voltage at time t, V_0 is the voltage amplitude and ω is the radial frequency [rad s^{-1}].[53]

$$V(t) = V_0 sin(\omega t) \tag{2.6}$$

The relationship between radial frequency and frequency f[Hz] is $\omega = 2\pi f$. The variation in the applied voltage will induce a current response which is a sinusoid with the same frequency, but shifted in phase. The current response can be expressed by equation 2.7, where I(t) is the current at time t, I_0 is the current amplitude and Φ is the phase shift.[53]

$$I(t) = I_0 sin(\omega t + \Phi) \tag{2.7}$$

The impedance is defined as the ratio of the voltage and current, see equation 2.8. The impedance has both a magnitude $Z_0 = \frac{V_0}{I_0}$ and a phase Φ, i.e. it is a vector. It is also often presented as a complex quantity.[53][54]

$$Z = \frac{V(t)}{I(t)} \tag{2.8}$$

Electrical resistivity is a measure of how strongly a material opposes the flow of electric current. It is a specific material property with the SI unit Ωm. Resistivity can be calculated from a measured resistance value, provided the cross-sectional areal (A) and thickness (l) of the conducting material is known, see equation 2.9.

$$\rho = R\frac{A}{l} \tag{2.9}$$

2.4.2 EIS as applied to Organic Coating Systems

Electrochemical systems are often modelled using so called equivalent circuit elements. That is, the electrochemical system is considered a series of simple electrical elements: resistances, capacitances, inductances, etc.[54] A perfect organic coating, can be modelled as a capacitor with capacitance of $C_g = \epsilon_0 \epsilon_r \frac{A}{l}$, where ϵ_r is the dielectric constant of the coating, A is the area of coated metal and l is the thickness of the coating.[53]

A non-perfect coating can be modelled by a more complex system, shown in figure 2.3.[53] Here, the capacitance called C_g is in paralell with a resistor (R_{Bulk}). This

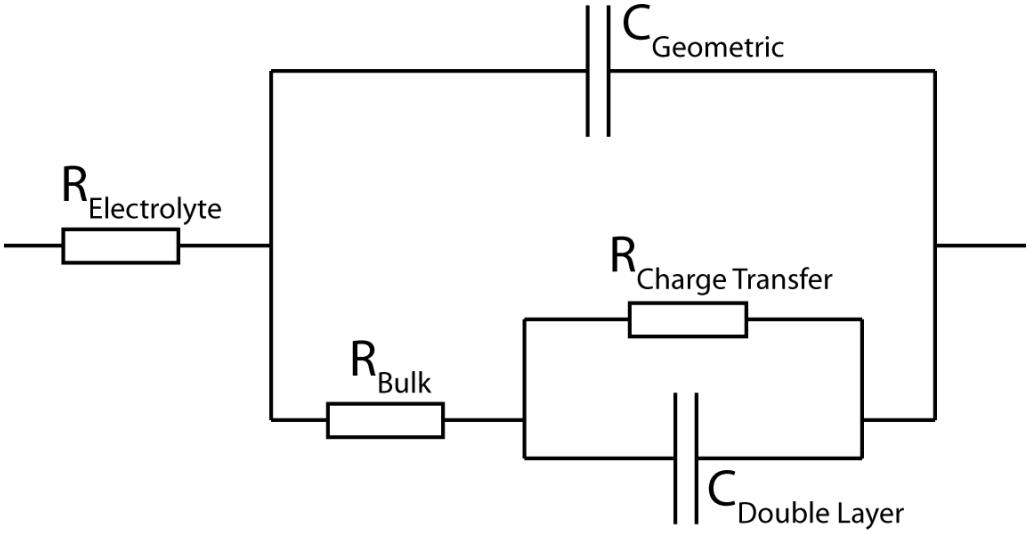

Figure 2.3: Equivalent circuit for a non-perfect coating

bulk resistance represents ionic transport occuring through the coating, for a perfect coating this resistance would be infinite. In series with R_{bulk} we find R_{ct} and C_{dl} in paralell. R_{ct} represents the resistance of the charge transfer itself, also called faradaic impedance. C_{dl} is the capacitance of the electric double layer. The importance of this double layer and the effect coatings have on it was discussed in section 2.1.2. In addition to these another resistor, R_e coupled in series with the system shown in figure 2.3, is sometimes considered. R_e represents the resistance offered by the electrolyte itself. The size of R_e usually makes it insignificant compared to the rest of the system.

The different circuit elements will react differently to perturbations of different frequencies. For very high frequencies the impedance of a capacitor goes towards zero, for very low frequencies the impedance of a capacitor goes towards infinity.[53] Thus, at high frequencies the AC current will short out through the capacitors, and the resistors do not apply to the measured impedance. At low frequencies the impedance of the capacitors gradually increase until the current is completely dominated by the impedance of the resistors.[53] Results taken from very low frequency experiments (mHz range) will yield information about the bulk resistance and the charge transfer resistance, whereas experiments covering a larger spectrum of frequencies can give information about the system as a whole. Experiments performed at extremely high frequencies(MHz range) will only give information about the resistance offered by the electrolyte.

The three resistances present in the equivalent circuit (figure 2.3 are coupled in series. Hence, the largest resistance will dominate the measurements. The resistance of the electrolyte is several orders of magnitude smaller than the others and can be disregarded. Although the presensce of the coating will increase the resistance of the charge transfer reaction, the resistance of that reaction is also rather low to begin with. The resistance presented by bulk ion transport through the coating, on the other hand, is known to be high for commercial coatings on steel. Therefore impedance measurements at low frequencies will probably be dominated by the re-

sistance against ion transport. Coatings have been shown to have linear polarization curves, an indication that the resistance is dominated by ion transport through the coating, as opposed to charge transfer.[46]

A study of electrochemical impedance at different temperatures would reveal the ion transport properties of the coating products at these temperatures. A search of the available litterature has not revealed results from similar experiments performed on commercial coating products at temperatures above 100 °C, such values would be of great interest in the discussion regarding the suitability of coatings at these temperatures.

2.5 Heat Transport

Coated steel will, when exposed to a hot oil flow on the uncoated side and a cold electrolyte flow on the cold side, be subjected to a thermal gradient. The thermal gradient results from heat transfer from the oil, through the steel and the coating, to the electrolyte. Cathodic disbonding will propagate along the interface between the steel and the coating, it is therefore important to know the temperature at this interface. Brende presented a one-dimensional, steady state model of the heat transport relevant for this system in his master thesis.[38] (later published[33]) This model can be used to calculate the temperature at the coating-steel interface. The accuracy of the model was tested by equipping a sample plate with a temperature sensor, it was found to be adequate.[33] The most important points of the model are repeated below. The complete model is presented in appendix A.

Heat is transferred through the steel and the coating by conduction according to Fourier's law of heat conduction. The heat is transferred from the oil to the steel and then from the coating to the electrolyte through convection according to Newton's law of cooling. Through calculations of Reynold's number and Prandtl's number, both the oil flow and the electrolyte flow where found to be turbulent. The Nusselt numbers were calculated, the value of the Nusselt number yielded the convection heat transfer coefficient. Finally the thermal resistances of the discrete steps presented in figure 2.4 were calculated and the temperatures at the steel surface, the interface between the steel and the coating and at the coating surface were found. The results of these calculations, for an oil temperature of 150 °C and a coating dry film thickness of 700 µm is found in figure 2.5.

The steel coating interface is considered to be the most important area with regards to disbonding processes. If a neutral thermal gradient (i.e. the same temperature throughout) with a temperature equal to the calculated temperature at the steel coating interface presented in figure 2.5 is applied to a coating system, the the conditions at the interface will be the same. Experiments have shown that this nevertheless presents a much harsher environment for a coating system than what the positive thermal gradient presents.[3] The heat transport system must therefore be considered, because gradient-free systems correspond poorly to the gradient-reliant systems that occur in the field.

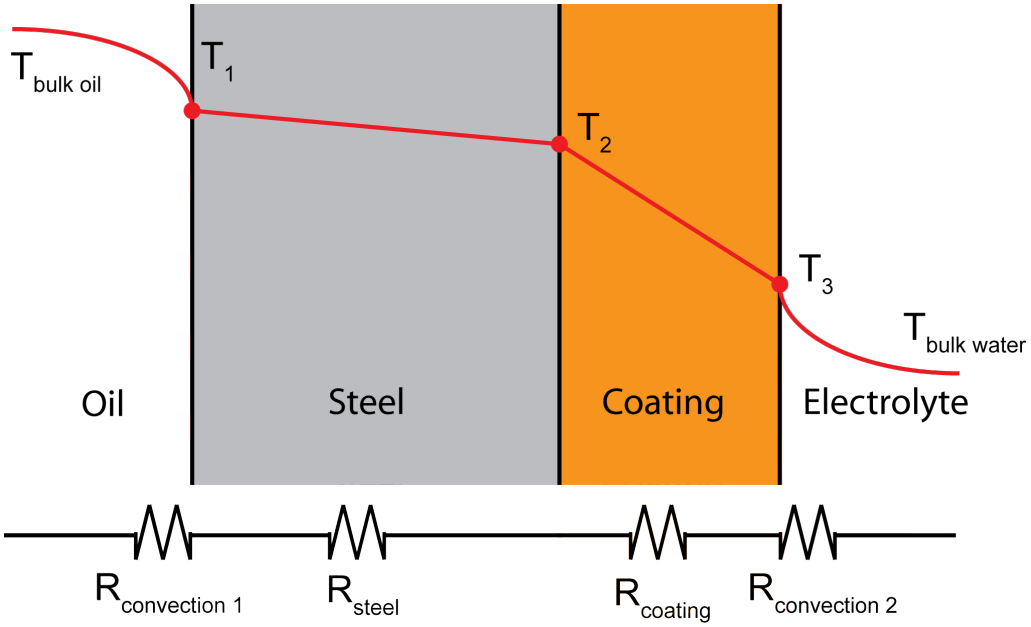

Figure 2.4: Heat resistance model and temperature profile, adapted from Brende[38]

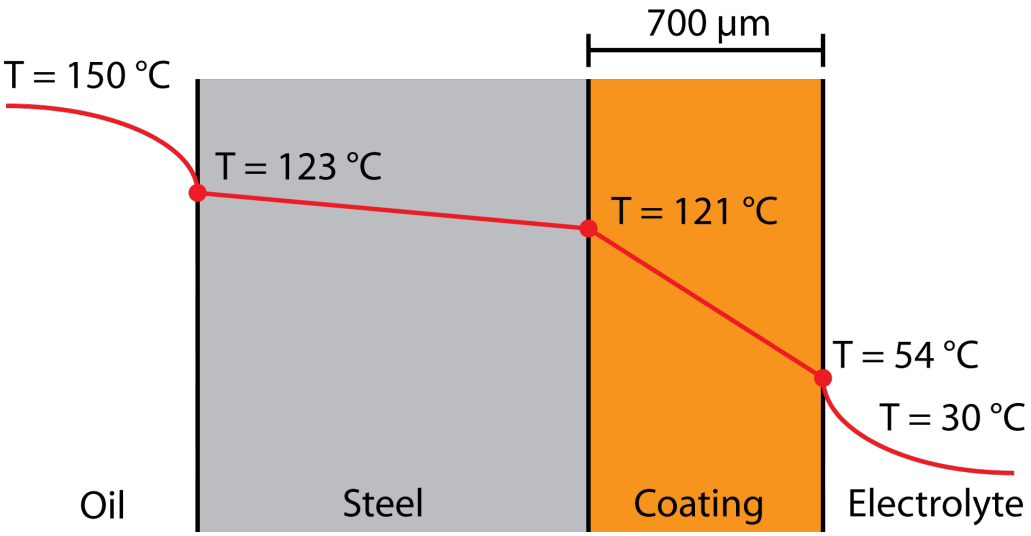

Figure 2.5: Calculated temperature profile

3 Experimental

3.1 The Sample Plates

The sample plates were made from st52 steel (DIN 17100, UNS G10150), measured 9.80 mm square and had a thickness of approximately 4 mm. Reasonable variation in the steel thickness has little relevance for the accuracy of the test, see appendix A. The sample plates were sent to different coating producers which freely chose pre-treatment methods, coating types and application procedures with the intention of creating a good candidate for high temperature, underwater exposure. The sample plates were equipped with an artificial holiday measuring 6 mm in diameter in the approximate center of the sample. The sample plates were connected to a potentiostat through a mechanically fastened wire. A sketch of a typical sample is shown in figure 3.1.

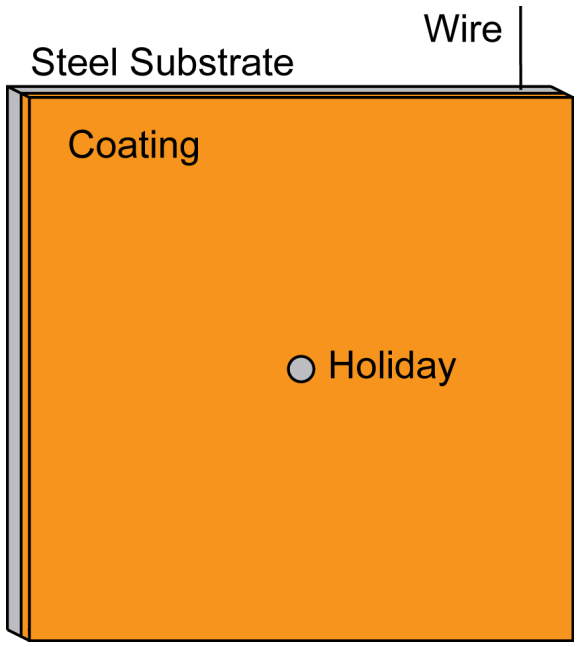

Figure 3.1: Coated Sample Plate

The tested sample plates were pre-treated and coated by a number of producers of organic coatings. A total of eight products were tested during this project. Seven of these products were tested in previous work by Brende, Knudsen and myself.[3][32][33][34][38] The same product designations (A through Q) were used in the cited studies, product R was not previously studied. The product designation, producer, generic type and average dry film thickness (DFT) of each product is presented in table 3.1 Product K was supplied by Exxon Mobile. Different batches of samples were used in the long term test and the shorter tests. Under the label DFT the numbers in the first column correspond to the average dry film thickness for each coating product in the batch used in the short tests, the numbers in the second column correspond to the average dry film thickness for each coating product in the batch used in the long term test.

Table 3.1: Overview of tested products

Designation	Producer	Generic Type	DFT [µm]	
			Short	Long
B	Jotun	Epoxy Amine Glass Flake	702	542
C	PPG	Epoxy Novolac	—	282
H	International	Epoxy Amine Glass Flake	1071	1035
I	Hempel	Bisphenol F	677	514
K	PPG/ExMo	Epoxy Novolac	660	657
N	International	Epoxy Novolac	1042	—
O	PPG	Epoxy Novolac	—	334
R	Carboline	Epoxy Amine	567	—
Control	—	Epoxy Mastic	221	

In addition to the eight tested products, one control system was tested. The control test was performed to evaluate the equipment with regards to bias based on the position of the sample in the equipment. Only the generic type and dry film thickness, as measured, of the control system is given in table 3.1.

Thickness measurements were performed with an Elcometer 256 FN T2 thickness measuring device, calibrated with Elcometer standard calibration films against a flat steel surface. A probe intended for ferromagnetic substrates and non-conductive coatings was used.

3.2 HTCD

3.2.1 The HTCD Apparatus

The high temperature cathodic disbonding (HTCD) apparatus was designed by Knudsen, Eggen and Brende[32]. It has since been used, either in its original form or with slight modifications, by Knudsen, Brende and myself.[3][33][34][38] A thorough description of the whole apparatus is included here for the sake of completeness.

The HTCD apparatus was designed to enable accelerated prequalification testing of organic coating products for immersion service on a hot steel substrate. The apparatus mimics field conditions to a certain degree, but several parameters have been changed to be more severe in order to accelerate any disbonding process. The field conditions the apparatus seeks to mimic involve a painted steel structure with cathodic protection immersed in relatively cool seawater and heated from the inside by a hot oil or gas flow from the reservoir.

The sample plates were mounted between two channels made from carbon steel, one containing a flow of hot oil, the other a flow of cool electrolyte. Circular holes were cut in the channel walls at the position of each sample plate, so that each sample plate was exposed to both flows. The oil channel was partially constricted with a

filler material, this decrease in the cross-sectional area increased the flow rate of the oil. The channel containing the electrolyte was painted on the inside and equipped with zinc anodes to protect it from corrosion. A Pt-wire clothed in a perforated plastic tube was drawn through the channel and used as the counter electrode. The interfaces between the sample plates and the channels were sealed with elastomer x-rings. The x-rings were insulating, ensuring that the sample plates were not in electrical contact with either channels or the zinc anodes. A cross section of a sample clamped between the two channels is shown in figure 3.2.

Fifteen sample plates were mounted simultaneously between the two channels. The whole two-channel system, including 15 samples and x-ring seals, is shown in figure 3.3. The oil was heated and pumped by a Tooltemp TT-360 oil heater. A regular hot-water tank was used as a heat exchanger to cool the electrolyte. A pump was used to provide the necessary electrolyte flow. The electrolyte was pressurized with air to prevent boiling at the hot interfaces. Previous results indicated that pressurization would be needed to achieve relevant results with oil temperatures above 140 °C[32], this was later confirmed.[3][33][34]. A schematic of the whole apparatus is shown in figure 3.4.

The sample plates were equipped with cathodic protection applied through a potentiostat. The ionic connection between the reference cell and the electrolyte in the channel (i.e. the salt bridge) was a combination of a high pressure part and an ambient pressure part. A wooden plug soaked in saturated KCl (aq) witheld the internal pressure in the equipment. A plastic tube filled with electrolyte and a soaked cotton thread connected the wooden plug to the reference cell. Standard calomel reference cells were utilized. The cathodic protection current was measured for each sample separately as a voltage over known resistances of 1 Ω each. The temperature was measured at the inlet and outlet of each channel throughout the experiment. A schematic of the electrical system is shown in figure 3.5. The potentiostats used were of the model Wenking MP 87. The data was logged with a Hewlett Packard 34970a Data Acquisition/Switch Unit.

During the 28 day experiment, a piece of zinc was exposed to the electrolyte flow. The zinc piece was used as the reference point for cathodic protection for a limited period. Measurements were made to compare the zinc electrode to the calomel electrode in an effort to determine the viability of using zinc as a reference electrode in the HTCD apparatus.

Cathodic protection was applied to the heat exchanger by a separate potentiostat to prevent pitting corrosion. A separate counter electrode was inserted in the heat exchanger. The same ionic connection was used for both cathodic protection systems.

3.2.2 The Long Term Test

A separate setup was used for long term testing. This equipment was not pressurized and did not utilize a closed electrolyte loop with a heat exchanger. Instead the long term test used seawater as the electrolyte, taken from Trondheim harbour (Norway).

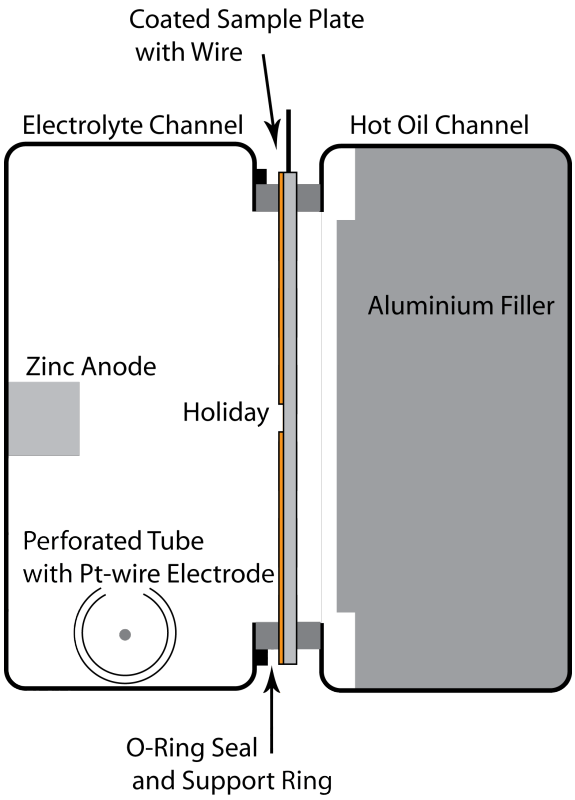

Figure 3.2: Cross section of the HTCD apparatus

Table 3.2: HTCD Test Plan

Test	$\mathbf{T}_{oil}$	**Products**							
		B	**C**	**H**	**I**	**K**	**N**	**O**	**R**
7 Days	150 °C	3	–	3	3	3	3	–	–
18 Days	150 °C	2	–	3	3	3	2	–	2
28 Days	150 °C	2	–	3	3	3	2	–	2
400 Days	120 °C	2	2	2	3	3	–	3	–
Control Test	100 °C	–	–	–	–	–	–	–	–

Apart from these differences the setup for the long term HTCD tests was identical to that of the short term experiment.

3.2.3 Experimental Program for the HTCD tests

A total of five tests were performed using the HTCD apparatus. Three of these were regular HTCD tests of various lengths, a 7 day test, an 18 day test and a 28 day test. In addition one 400 day long term test was performed with different parameters. A 7 day control test with 15 identical samples was also performed. The control test was performed to investigate wether the channel was unbiased, two identical sample plates should give the same disbonded distance, regardless of position in the test channel. Table 3.2 details how many sample plates were tested of each product in each test.

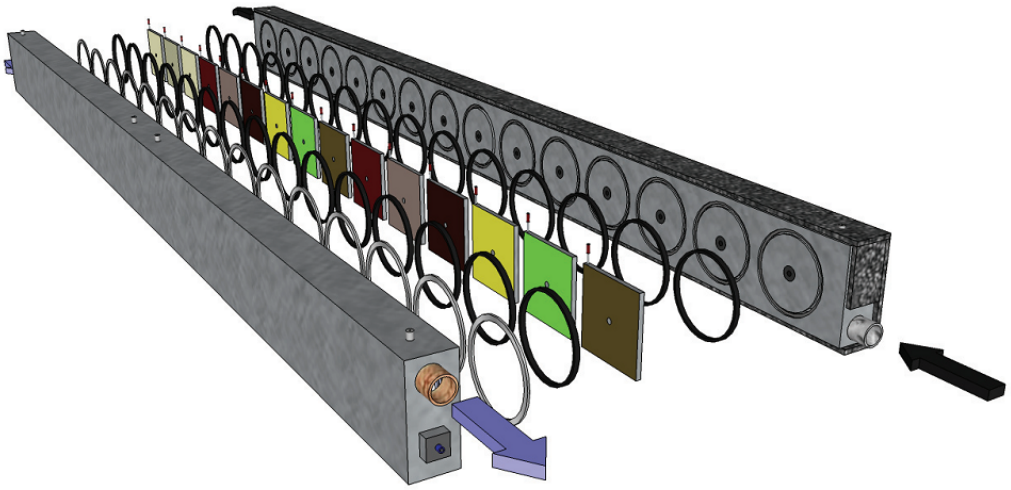

Figure 3.3: Sketch of the two channels

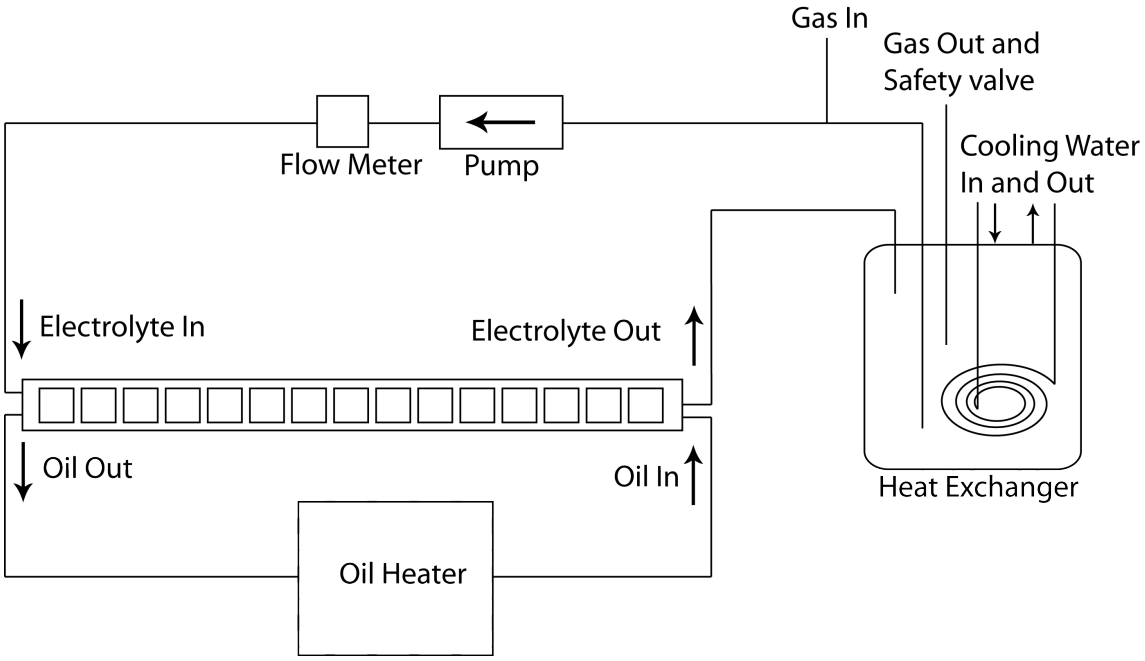

Figure 3.4: Schematic of the HTCD apparatus

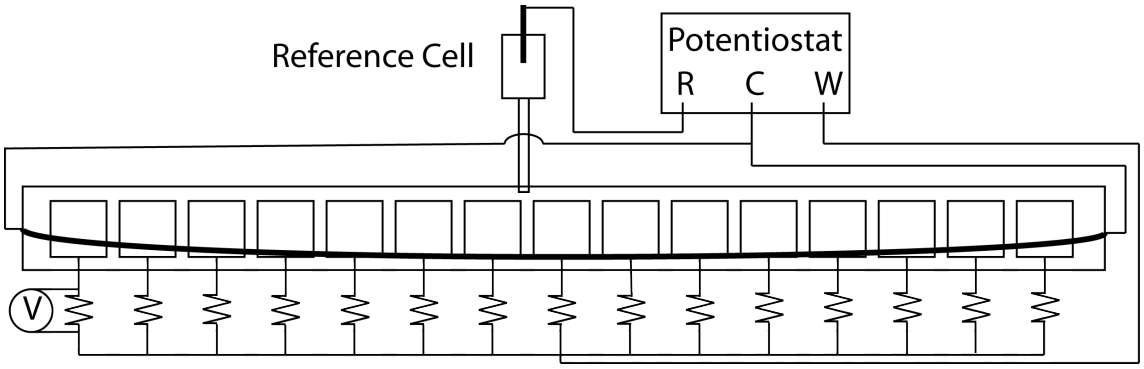

Figure 3.5: Schematic of the electrics of the HTCD apparatus

For the three regular tests, the temperature in the oil was 150 °C, the temperature in the electrolyte was 30 °C. The oil used was Hexatherm HT 22, a high temperature, low viscosity heat exchanger oil. The electrolyte used was aqeous 3.5 % NaCl. Additional data on the electrolyte and oil can be found in appendix A, Heat Transport Calculations. The equipment was pressurized with air to 3.5 Atm of overpressure, which corresponds to a partial oxygen pressure of 0.73 Atm. The samples were polarized to -1200 mV_{SCE}. The three tests had a duration of 7, 18 and 28 days respectively.

The long term test was performed with an oil temperature of 120 °C, the temperature in the electrolyte varied between 4 °C and 10 °C. The oil used was Shell Thermia B, a high temperature heat exchanger oil. The electrolyte was natural seawater, as collected from the Trondheimsfjord, in Trondheim harbour, Norway. The equipment operated at ambient pressure. The samples were polarized to -1100 mV_{SCE}. The test had a total duration of 421 days, of which 407 were heated; the experiment operated at ambient temperature the last 14 days due to difficulties with the oil heater.

The control test was performed with an oil temperature of 100 °C, the temperature in the electrolyte was 30 °C. The oil used was Hexatherm HT 22, a high temperature, low viscosity heat exchanger oil. The electrolyte used was aqeous 3.5 % NaCl. The equipment was pressurized with air to 3.5 Atm of overpressure, which corresponds to a partial oxygen pressure of 0.73 Atm. The samples were polarized to -1200 mV_{SCE}. The duration of the test was 7 days.

3.3 Oxygen Diffusion

The rate of cathodic disbonding is dependent on the concentration of oxygen[43][45] and the diffusion of oxygen through the coating is an integral part of the mechanism of cathodic disbonding.[1][2] As such, the diffusion speed of of oxygen in the relevant coating systems should be investigated.

An attempt was made to determine the diffusion coefficient of oxygen in the coatings by the delay-time method. Five of the coating products were tested in this manner.

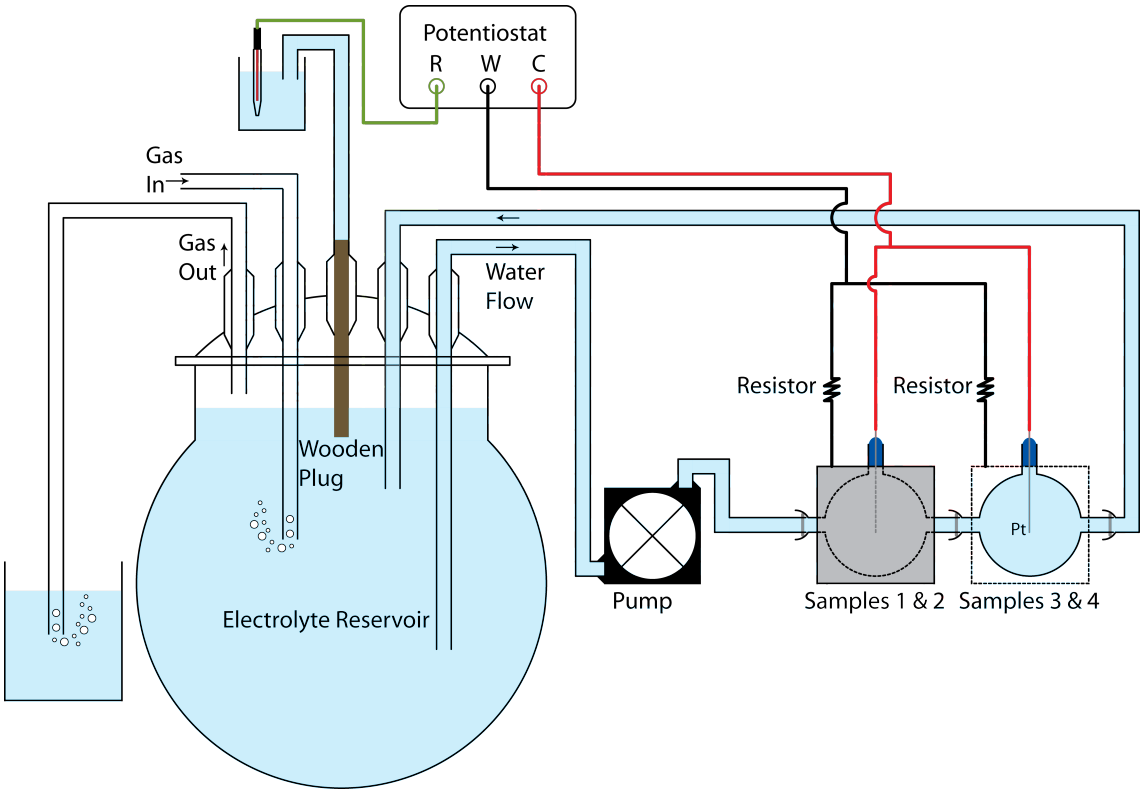

Figure 3.6: Setup for the oxygen diffusion experiment

The setup used was similar to the one described by Knudsen[2]. The sample plates were mounted in electrochemical cells that were connected in series forming one continuos electrolyte cycle. The sample plates were cathodically protected by a potentiostat applying a potential of -1.2 V_{SCE} for the first 24 hours, later lowered to -1.8 V_{SCE}. The necessary protection current for each sample was measured by observing the potential drop over a resistor of 1 MΩ. The exposed area of each sample plate was 19.6 cm^2. The electrolyte (3.5 w% NaCl (Aq)) was circulated through the cells and a larger reservoir. Nitrogen gas was bubbled through the electrolyte reservoir for some time to remove any oxygen present. A lack of oxygen could be observed through the necessary protection current. Once the protection current was stable, the electrolyte was saturated with air. The current was measured with the intention of calculating the diffusion coefficient based on the break-through time as presented in equation 3.1[2]. The setup used is presented in figure 3.6.

$$D_{O_2} = \frac{\delta^2}{15.3 t_b} \tag{3.1}$$

The measured currents were extremely low, on the pico ampere scale. Consequently the whole experimental setup was placed inside a Faraday's cage to shield it from electromagnetic noise.

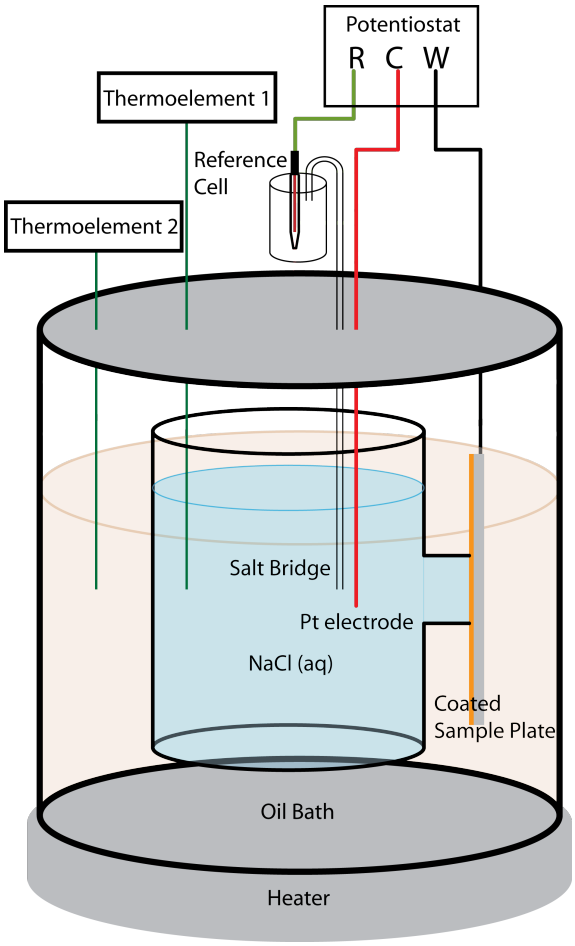

Figure 3.7: Setup for EIS in Autoclave

3.4 Electrochemical Impedance Spectroscopy

Some of the products were tested using electrochemical impedance spectroscopy. The samples were mounted in an electrochemical cell, which in turn was immeresed in an oil bath to provide heating. The cell and oil bath were placed inside an autoclave to enable heating beyond the boiling point of water. The setup is illustrated in figure 3.7. The conditions were similar to those used in the HTCD tests. The electrolyte was an aqeous, 3.5 % NaCl solution. The samples were polarized to -1200 mV_{SCE}. An alternate current of 10 mHz with an amplitude of 10 mV was impressed on the system. Impedance measurements were performed at intervals between 30°C to 150°C. Insulating transformer fluid was used for the oil bath. A Zahner IM6 with a high impedance probe was used to perform the measurements.

The exposed area was circular with a radius of 10 mm. The thickness of the different coatings were measured with an Elcometer 256 FN T2, calibrated against a flat steel surface, a probe intended for ferromagnetic surfaces and non-conductive coatings was used. The thicknesses were as follows: H, 1112 µm, I, 678 µm, K, 718 µm, N, 912 µm. Using these values the bulk resistivity of the various coating products was calculated at different temperatures.

3.5 Scanning Electron Microscopy

A scanning electron microscope (SEM) was employed to investigate the cross section of a sample plate. A sample was tested in the HTCD apparatus as part of the 18 day test. After exposure to the HTCD environment, the plate was cut in half, with the cut passing through the holiday. Half of the sample was evaluated in the usual manner. The other half was embedded in an epoxy resin. The cross section was ground and polished, and a thin layer of carbon was applied by sputtering.

After preparation as a SEM-sample, the cross section was studied in a Hitachi 3400N LVSEM, the accelerating voltage used was 15 kV. Secondary electrons were used for the general imaging. Energy-dispersive X-ray Spectroscopy (EDS) was used to analyze the chemical composition of the salt deposits present in the holiday, and along the coating-substrate interface. EDS was not employed on the coating itself.

4 Results

4.1 HTCD

The disbonded distance and disbonded area is listed for each coating product for each experiment in table 4.1. Figure 4.1 presents these results graphically, where samples marked 'X' failed and samples marked '–' were not tested. Figure 4.2 displays the relation between time and disbonded area more clearly for each of the six most widely tested coating product. Images of some of the tested samples are included in appendix D.

Table 4.1: Results from the HTCD Test

	Distance [mm]				**Area** [mm^2]			
Time [Days]	**7**	**18**	**28**	**400**	**7**	**18**	**28**	**400**
Product B	0	6.5	5.56	X	0	255	202	X
Product C	–	–	–	5.59	–	–	–	204
Product H	0.46	11	6.65^b	2.78	9	587	264^b	77
Product I	0.83	2.79	2.58^a	2.31	18	77	70^a	60
Product K	1.71^a	5.92	5.38^a	1.91^a	41^a	222	192^a	47^a
Product N	1.71	6.34	6^a	–	41	246	226^a	–
Product O	–	–	–	X^b	–	–	–	X^b
Product R	–	2.16	1.97^a	–	–	55	49^a	–

^{a} — the sample showed blisters in the disbonded area
^{b} — the sample showed blisters outside of the disbonded area
X — the sample suffered from complete loss of adhesion
– — the sample was not tested

The 18 day test resulted in a larger disbonded area than the 28 day test for all the tested coating products. This was likely due to experimental error involving a problem with the salt bridge connection to the reference cell. Caution is adviced, if conclusions are to be drawn based on the results from the 18 day test.

Some samples suffered from blistering. Product H showed severe blistering in the 28 day test, where large blisters were formed far from the holiday, outside of the disbonded area. Product O suffered from blistering in the 400 day test, the blisters were spread over the whole sample area. Blisters were also observed on other samples, but these observations were confined to the disbonded area of the coating.

Product B showed a very non-standard extent of disbonded area in the 400 days test. Product B still showed adhesion in a radius up to several centimeters around the holiday, but was completely disbonded along the outer edges of the exposed area. No other products showed this result and both samples of product B showed the same result. In the 28 day test the two samples of product B only showed partial disbonding. An outer layer of the coating disbonded easily, while the innermost layer stayed bonded to the substrate. This may have been a case of the second coat delaminating from the first coat, which sometimes occurs when autoadhesion fails prior to coating-substrate adhesion failure. The resulting surface was uneven.

Several samples from the 18 day test were severely attacked along the edge of the exposed area. The damage did not extend all the way from the edge to the holiday, but rather covered the area close to the edge, disbonding could therefore be determined in the usual manner near the holiday. Problems with the salt bridge to the reference cell during the 18 day test resulted in a very high cathodic protection current, which led to extensive hydrogen evolution on the cathodes and hypochlorite evolution on the anode. Examples of sample plates with clearly visible attack along the edge are included in appendix D.

As was noted in section 2.2.2, assessing the disbonded area under very thick and hard coatings can be difficult. The alternate method described in section 2.2.2, utilizing a knife and mallet, was used for some of the samples. A series of samples from the 28 day test were tested in the usual manner, scalpell lift-off, on three quarters of the holiday circumference, while the final quarter was tested with the alternate method. The two test methods showed adequate correlation, the method is detailed in appendix C, where images of the dual-test samples are included.

If a linear relationship, after the initiation period, is assumed according to the current theory, see section 2.2.3, area as a function of time can be found by linear regression from the measurepoints in figure 4.2. For reasons discussed in section 5.1.2 only products H, K and N were included, and only the results from the 7 and 28 day tests were used for the regression. The regression is presented in figure 4.3. The initiation period for the coating products, according to this model, was 159 hours for product H, 29 hours for product K and 55 hours for product N.

The required protection current for each sample was logged during each test. The total protection current from the 28 day test, for all 15 samples combined, is included in figure 4.4. In the course of the test the electrolyte was changed several times, and the salt bridge to the reference cell had problems at one point; discontinuities in the graph corresponds to electrolyte changes and periods with connection problems. The protection current for individual samples can be found in figure 4.5, note that the scale of the graph has been greatly reduced, compared to figure 4.4, to make it easier to differentiate between the samples. Only the results from the 28 day test are included here, similar results were observed in all the tests.

The potential of the solid zinc reference electrode was monitored throughout the 28 day test. The potential was found to vary between ~-1280 mV_{SCE} and ~-1210 mV_{SCE}. More deviant potentials ranging from -1320 mV_{SCE} to -1050 mV_{SCE} were observed for short periods. The variation did not correlate with a change in any other observable parameters.

4.2 Oxygen Diffusion

The initial values for the protection current were quite low, in the order of 10 to 100 pA. These values did not change significantly with time. The values are presented graphically in figure 4.6a. Note that the sudden, permanent increase in current after 24 hours was caused by a lowering of the applied potential from -1200 mV_{SCE} to -1800 mV_{SCE}.

After a period of observing the protection currents without noticing any change, the system saturated with air. The protection currents seemed unaffected by the presence of air in the electrolyte, this is presented in figure 4.6b where time 0 is the time of aeration.

Two parallels of each of five coating products (B, H, I, K, N) were tested. The results of the two parallels of each coating product correlate well, indicating that the test results were not dominated by random noise. Note that the noise in the areas between 90 and 100 hours in figure 4.6a and that at about 23 hours in figure 4.6b were caused by external disturbances. The low current levels made the experiment vulnerable to electric noise.

4.3 Electrochemical Impedance Spectroscopy

The tested coating products yielded quite high impedance at room temperature, but these dropped sharply upon heating to 30 °C. Upon heating to higher temperatures the impedance was even more reduced. Only products I and N were tested above 100 °C. Product I showed reduced impedance up to about 140 °C where it reach a stable level. Product N seemed to reach a somewhat stable level at 100 °C, with no distinctive reduction in impedance above this temperature. The measured values at the 10 mHz frequency are shown in figure 4.7a. The same general trend is evident when the measured values are corrected for exposed area and coating thickness, i.e. when the bulk resistivity of the coating is considered. This is shown in figure 4.7b

Polarization curves were recorded for all the coating products included in the EIS experiment. The polarization curves were linear, indicating that the resistance is dominated by ion transport, as opposed to charge transfer resistance.

During the Electrochemical Impedance Spectroscopy it became evident that the impedance was affected by the thermal history of the sample. Samples that had been previously heated to elevated temperatures showed lower impedance at ambient temperatures compared to samples that had not been subject to the same heating. Figures 4.8a and 4.8b show the measured effect for product I and N. The values measured at 30 °C after previous heating to 100 °C are a decade lower than those measured at 30 °C with virgin samples, corresponding to the values measured between 60 °C and 90 °C for virgin samples. Values measured at 50 °C after previous heating to 100 °C are very close to those measured at 30 °C after previous heating. Note that after the heating the samples were stored for at least 24 hours before they were tested at ambient temperatures. Disturbances near 50 Hz are caused by the power grid (the power grid in Norway operates at 50 Hz) and should be ignored.

4.4 Scanning Electron Microscopy

The scanning electron microscope (SEM) allowed the study of several features; the steel substrate, oxide deposits on the substrate surface and along the substrate coating interface and the coating itself including pigments and voids were all successfully

imaged in the SEM. An overview of the cross section is presented in figure 4.9. The lower part of the image is the steel substrate, the upper right part is the coating, where voids are easily visible, the upper left part is the holiday. In the corner where the three distinct parts meet there is an oxide inclusion; carefull examination also reveals oxide inclusions along the coating-substrate interface.

The coating and substrate are distinctively different, which makes determination of the interface between the two easy. In regions where disbonding has occured a small crack, often accompanied by oxide deposits, is visible along the interface. In regions outside the disbonded area the interface is clean, free of cracks and deposits. See figures 4.10a and 4.10b for examples of the interface in an area with disbonding and in an area without disbonding. The difference between the disbonded and the intact interface allowed the extent of disbonding to be determined by SEM-images, it was found to be ~1200 µm.

Electron-dispersive X-ray spectroscopy (EDS) was used to determine the composition of the oxide deposits. EDS revealed the oxide in the holiday to be mostly calcium oxide and zinc oxide. Some of the deposits on the coating-substrate interface near the holiday were also found to consist of calcium oxides and zinc oxides. Deposits further away from the holiday consisted of iron oxide. EDS spectra from these locations are included in appendix F. The coating itself was not studied with EDS.

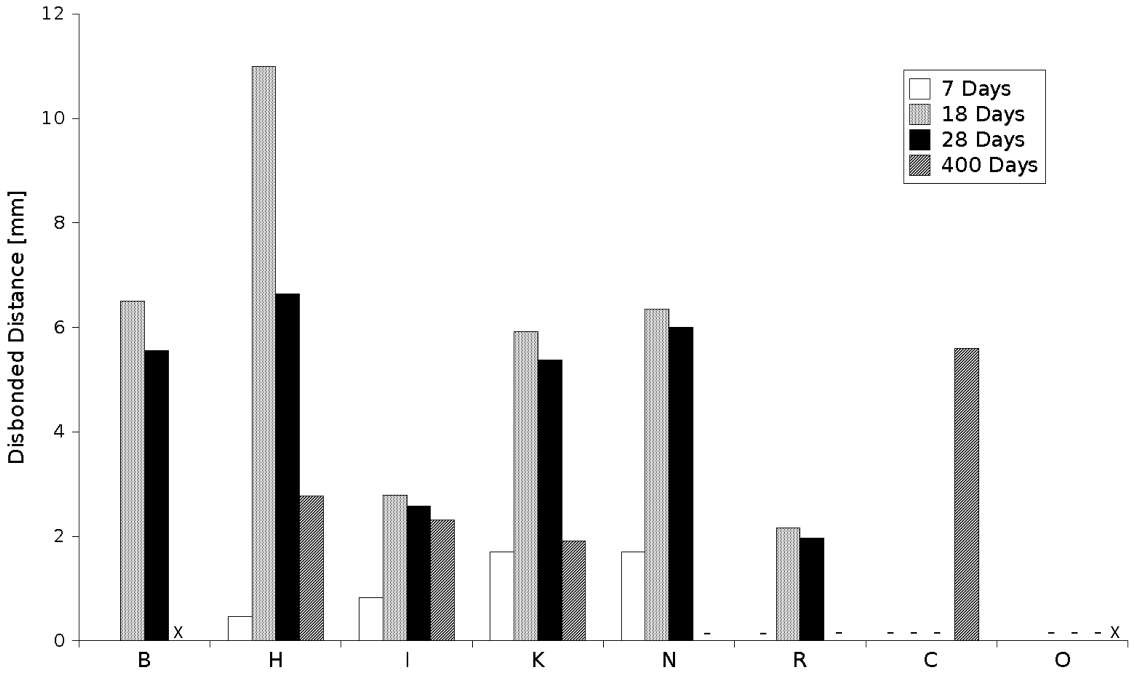

Figure 4.1: Disbonded Area by Product Code

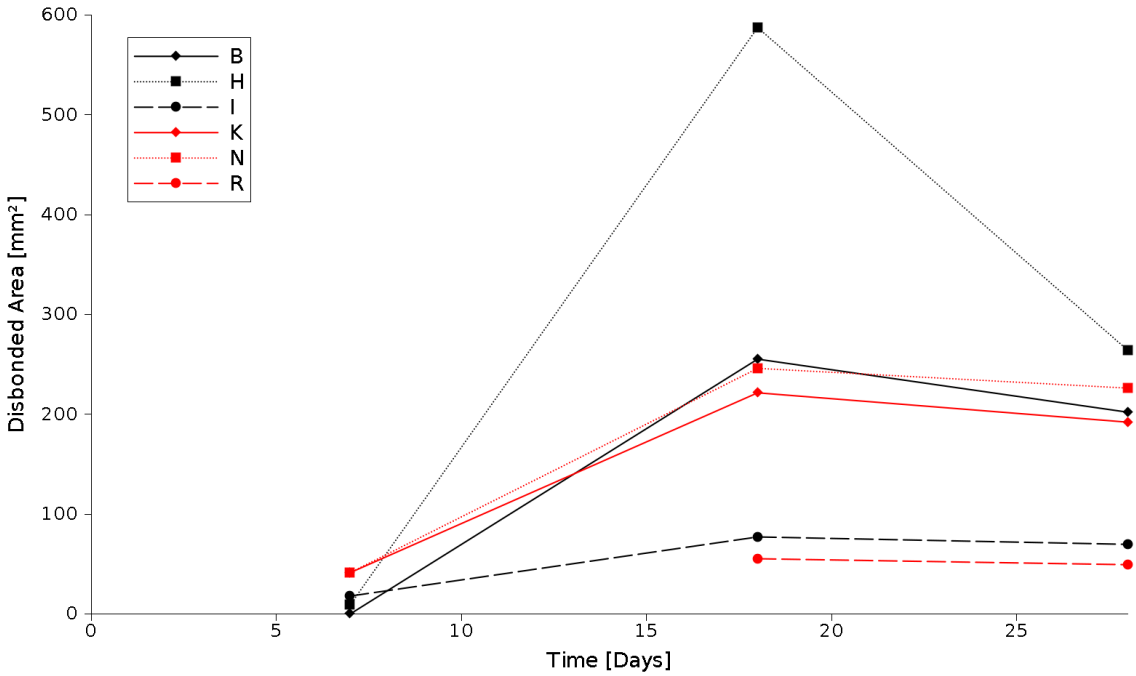

Figure 4.2: Time Dependency of Disbonded Area

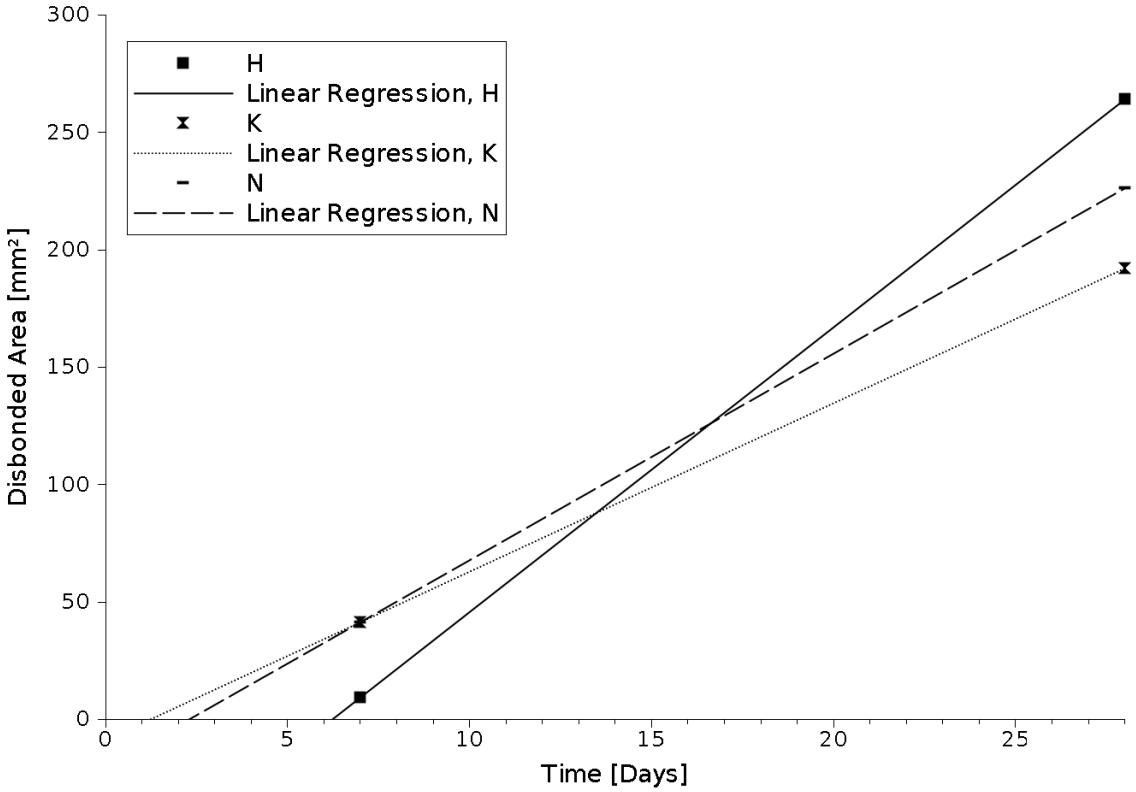

Figure 4.3: Linear Time-Area Relation

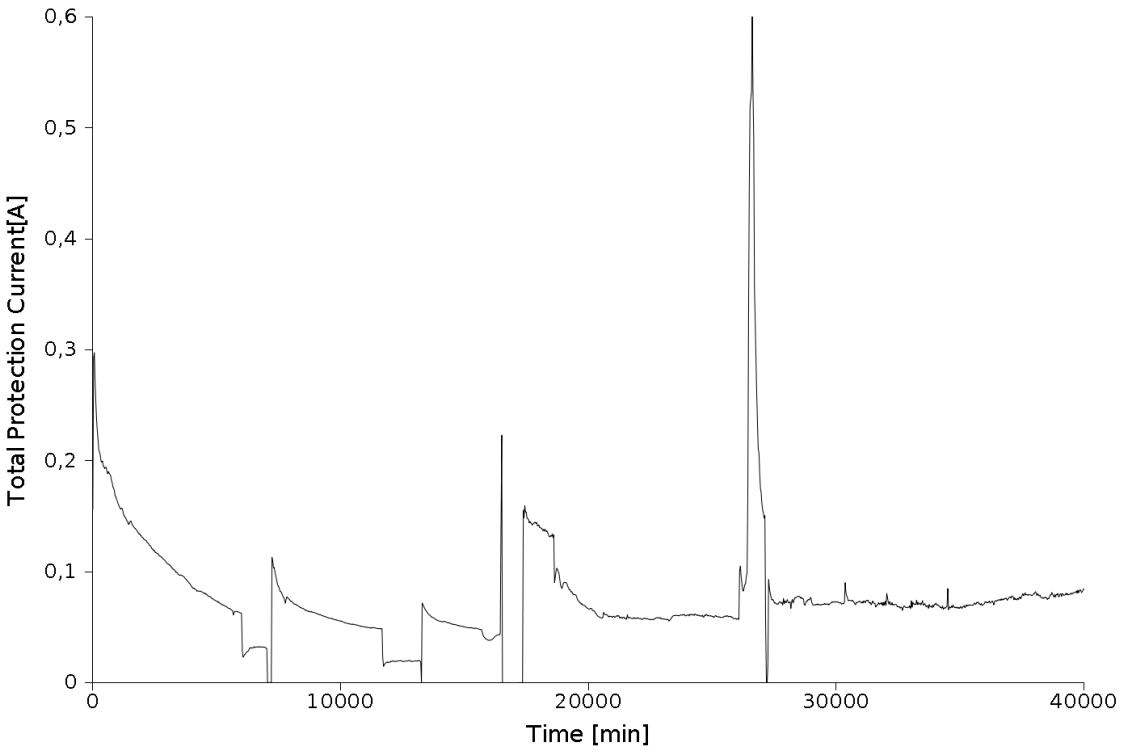

Figure 4.4: Total Protection Current, 28 Day Test

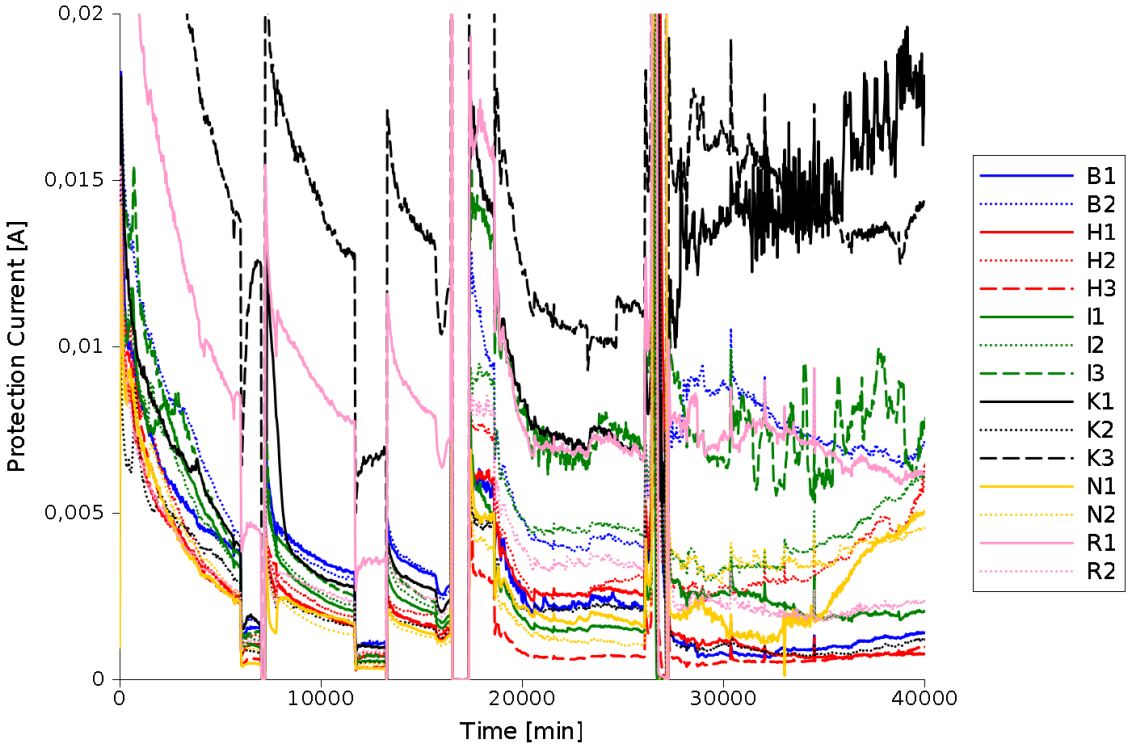

Figure 4.5: Protection Current, 28 Day Test

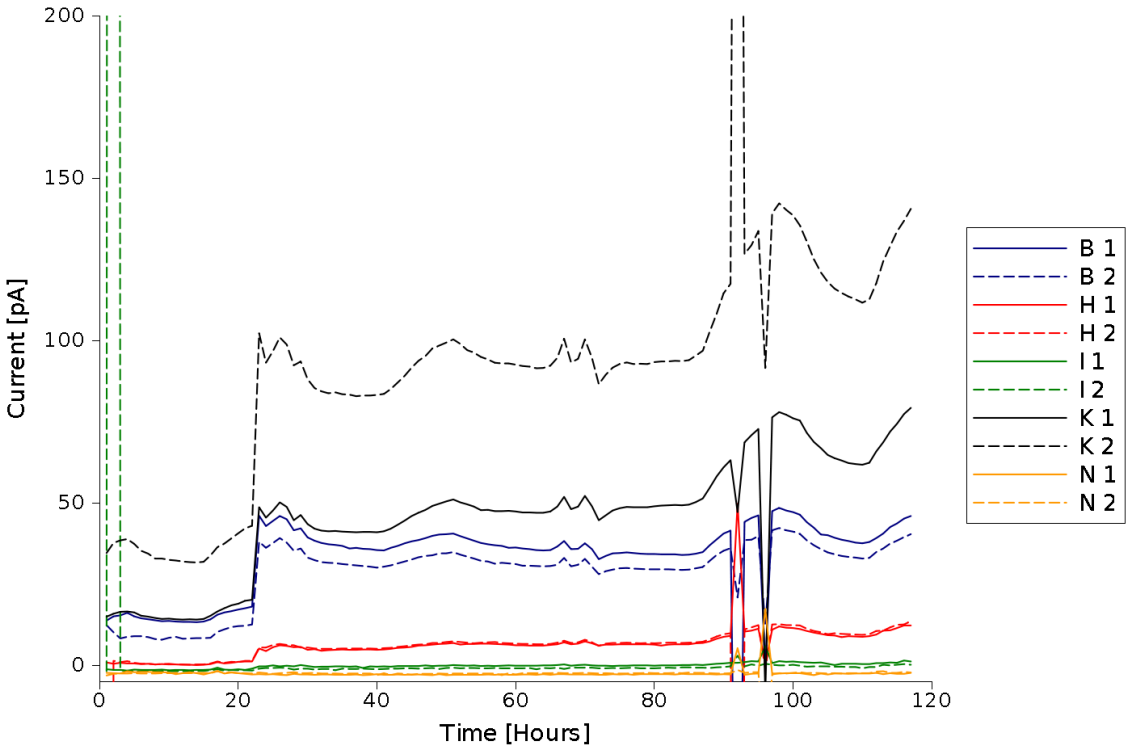

(a) Before Aeration

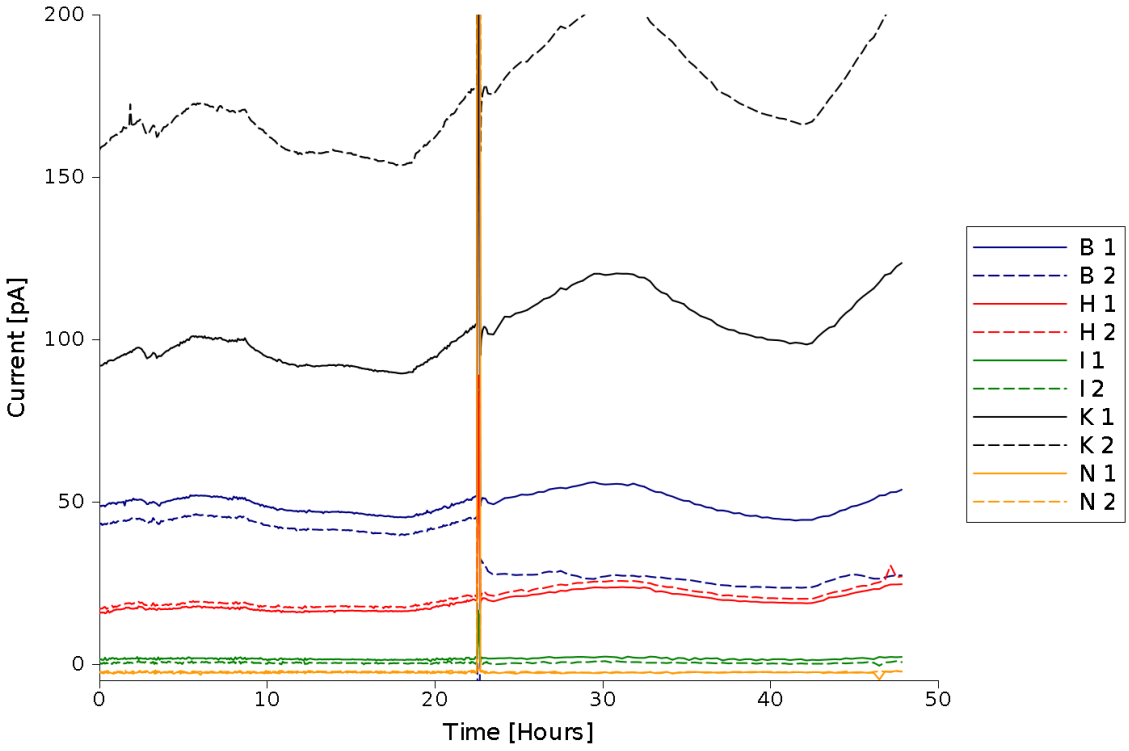

(b) After Aeration

Figure 4.6: Current Measurements from the Oxygen Diffusion Experiement

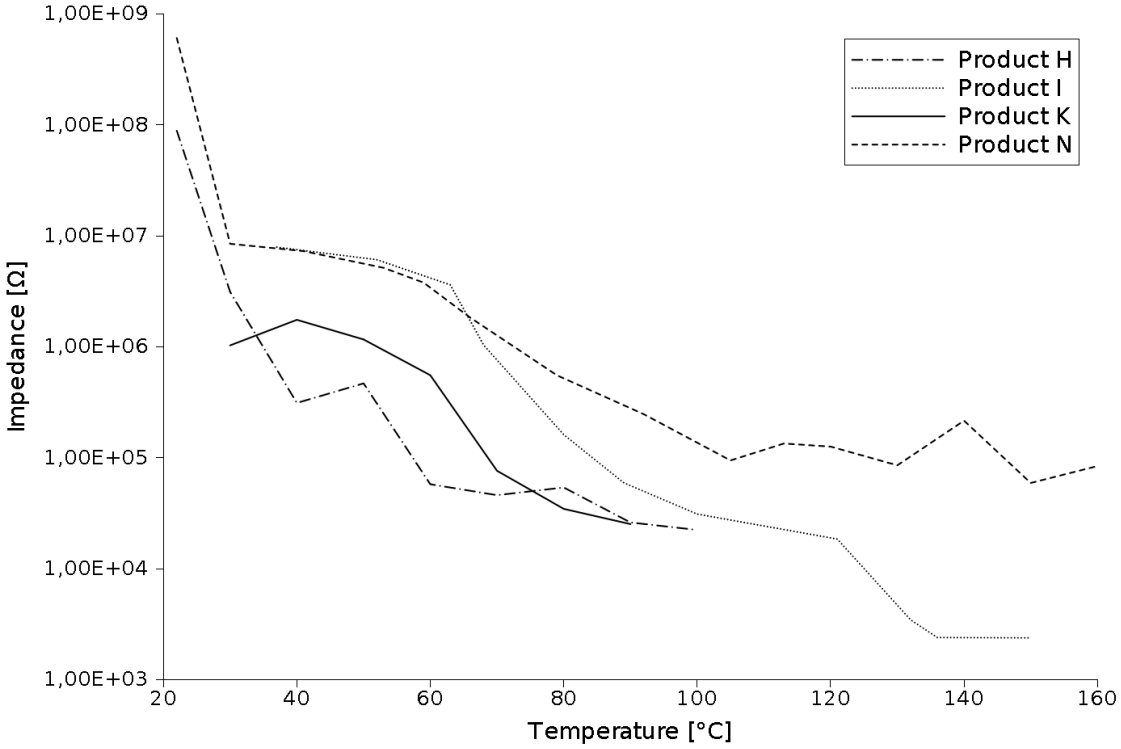

(a) Impedance

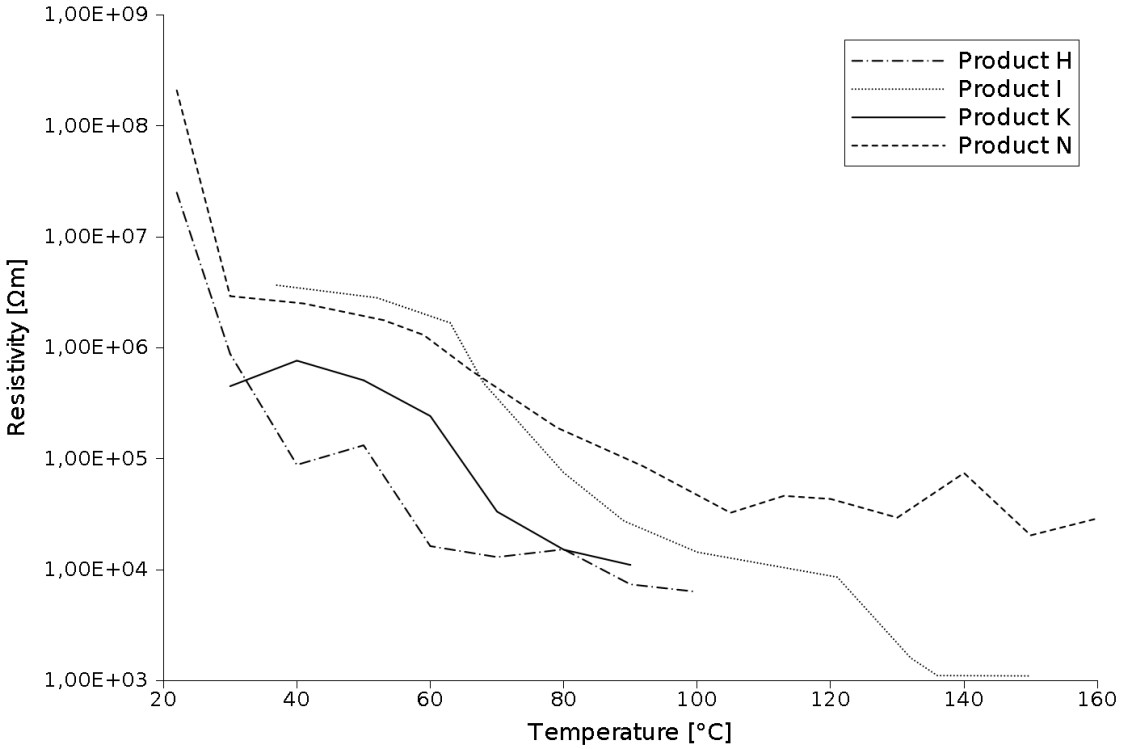

(b) Resistivity

Figure 4.7: EIS Results, 10 mHZ

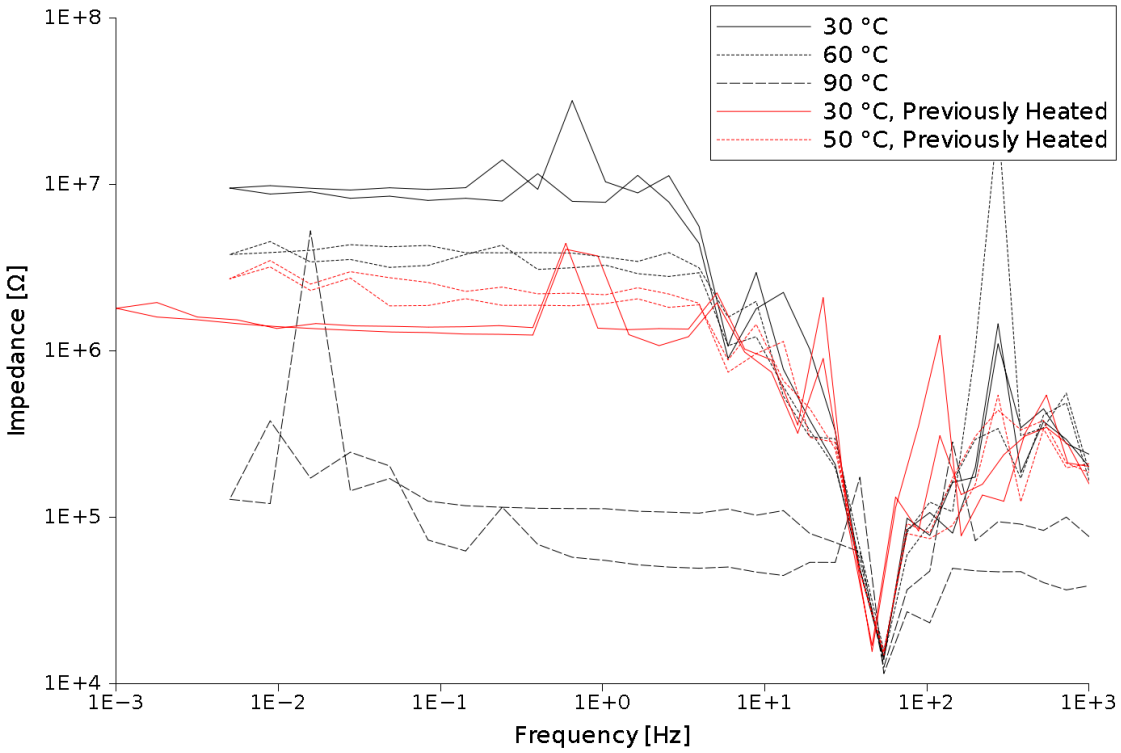

(a) Product I

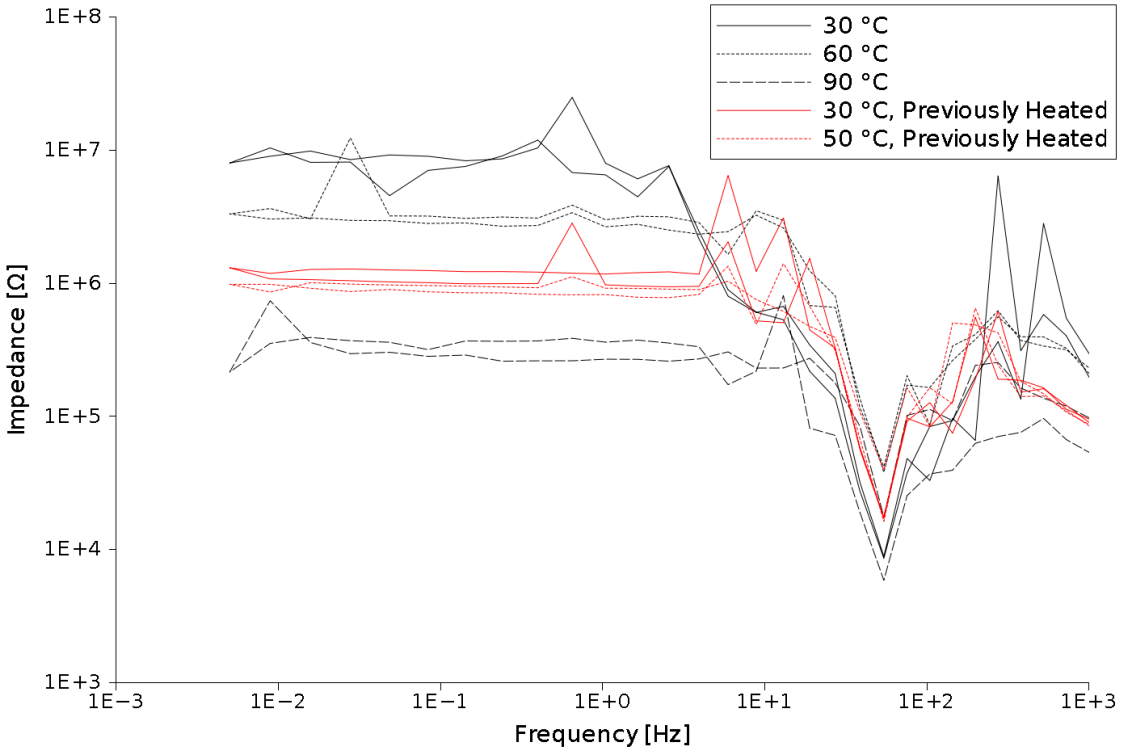

(b) Product N

Figure 4.8: EIS with Previously Heated Samples

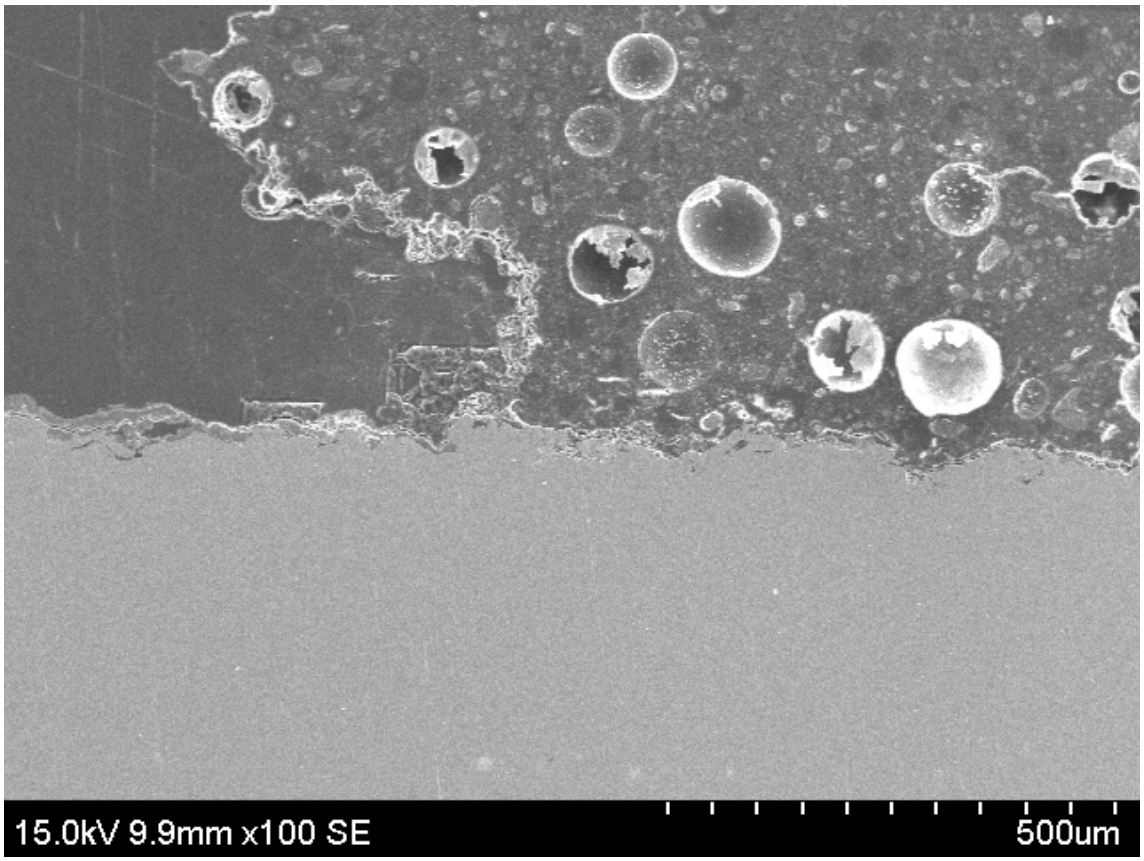

Figure 4.9: SEM Holiday Overview

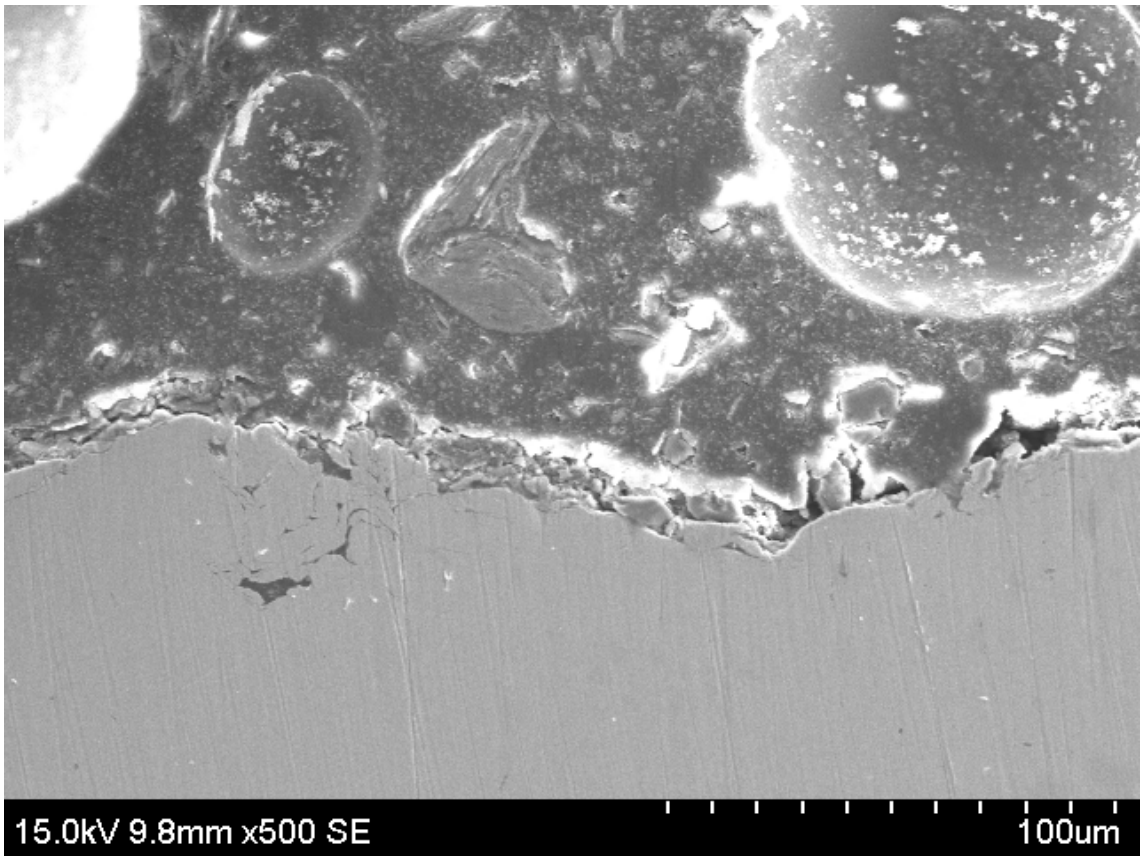

(a) Disbonding

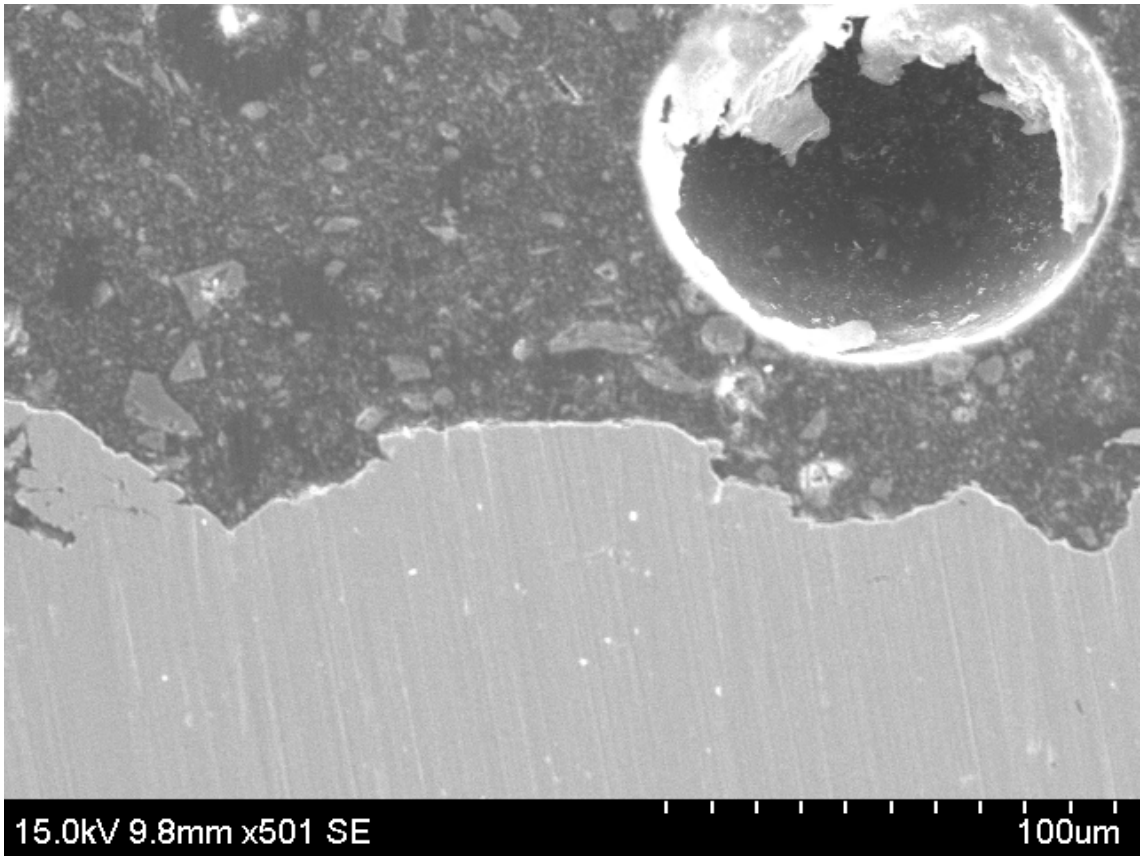

(b) No Disbonding

Figure 4.10: Coating-Substrate Interfaces

5 Discussion

5.1 HTCD

5.1.1 Product Performance

Some of the coating products tested were previously tested using the same equipment, these results are included in appendix B. Coating product H and I performed well in one week tests with oil temperatures ranging from 120 °C to 180 °C. B, K and N also performed well in the temperature range up to 160 °C. No tests with an oil temperature of 150 °were performed in the previous work. Product R had not been previously tested. All temperatures mentioned in this section refers to oil temperature, the temperature of the steel and that of the electrolyte was lower than the oil temperature, see section 2.5 and appendix A for the relationship between the oil temperature and other important temperatures.

Product B performed extremely well in the lower temperature tests (120 °C and 140 °C). In the 160 °C test it suffered from complete loss of adhesion in the exposed area. In the most recent tests, at 150 °C, product B showed no signs of disbonding in the 7 day test, but moderate disbonding in the 18 and 28 day tests. Product B showed disbonding all the way out to the edge of the exposed area in the 400 day test, but it still showed good adhesion immidiately adjacent to the holiday. The crevice beneath a disbonded coating film presents an extremely harsh chemical environment with a high pH, high temperatures and stagnant flow conditions. It is possible that the the actions of this environment has caused the binder, pigments or some other component in the coating to break down and form a sticky mass which allowed readhesion. Since the disbonded area extended far beyond the area that still showed adhesion, it can be concluded that this readhesion did not protect the substrate as well as an intact coating would. Knudsen has observed similar results previously and, at the time, considered chemical breakdown, followed by readhesion, to be the best explanation.[55] Cathodic disbonding can give pH values as high as 14 beneath the disbonded coating[1], this is high enough to damage many types of glass(product B is pigmented with glass flakes) and some types of epoxies. Given the observed results it seems likely that product B suffers from partial breakdown after exposure to the environment present beneath the disbonded coating.

Product H performed excellently in the previous tests, but gave significant disbonding in the 18 day test, while some samples suffered from severe blistering in the 28 day test. Nothing similar was observed in the previous tests performed at 160 °C and 180 °C, which showed that product H can sustain high temperatures for 7 days. The results from the 18 and 28 day tests suggest that product H is not suited for long term exposure with oil temperatures as high as 150 °C. Product H is very thick, it has the highest dry film thickness of all the tested products. The great thickness of the coating may contribute to a lengthy onset time for any degradation mechanism, after which degradation propagates at a quick pace. This would explain the relatively poor performance in a 4 week test at 150 °C compared to excellent performance in 1 week tests performed at higher temperatures. Product

H performed very well in the 400 day test at 120 °C, this suggests that the coating product is well suited for use on moderately hot, submerged steel structures.

Product I performed excellently previously in the 7 day tests at 140 °C and 160 °C, it also performed very well in the 7 day test at 150 °C. Product I displayed the same excellent performance in the longer tests showing only very limited disbonding in the 18 day and 28 day test, as well as the 400 day test at 120 °C. Product I is an excellent candidate for high temperature underwater use.

Product K gave moderate disbonding in the tests at 140 °C and 160 °C. It gave the most disbonding of all the tested products in the 7 day test, though it is important to note that this is measured relative to other excellent coatings and that the measured disbonding, on an absolute scale, is very limited. Product K showed moderate disbonding after the 18 and 28 day tests, with cracking present on one sample in the 28 day test. Since only one sample showed cracking, and this was not observed in tests at 160 °C, it is likely that this was an atypical result. Coating systems are inherently heterogenous and many factors can contribute to unexpected failure. Product K showed very limited disbonding in the 400 day test.The results indicate that product K may not be suited for exposure to the highest temperatures, but like product H, is well suited for moderately hot surfaces.

Product N performed extremely well in the lower temperature tests (120 °C and 140 °C). In the 160 °C test it suffered from some cathodic disbonding. It showed moderate disbonding in all the tests performed at 150 °C. Product N was not included in the 400 day test. Product N is a very hard and tough coating system and is excessively difficult to assess with the standard method, but it is easy to test with the alternate method presented in appendix C as it has displayed a clearly visible, black, discoloration beneath the disbonded coating in all tests. Since it is difficult to remove the disbonded coating without breaking multiple scalpels it is perhaps timely to discuss whether this can be regarded as breakdown at all. The coating is still very difficult to remove, the protection current does not increase significantly and the substrate remains relatively intact. With this in mind, product N can be recommended for high temperature underwater use, despite showing some disbonding in the tests.

Product R was not previously tested, neither was it included in the 400 day test. It performed excellently at 150 °C, showing no disbonding in the 7 day test and only very limited bonding on the 18 and 28 day tests. Product R is an excellent candidate for high temperature underwater use.

Products C and O both performed quite poorly in the tests at 120 °C and 140 °C and failed completely at 160 °C. For this reason they were not included in the tests performed at 150 °C. They were however included in the 400 day test where product C gave a large disbonded area and product O failed by blistering.

All samples included in both the 18 day test and the 28 day test performed better in the 28 day test. This is likely an experimental error. As noted in section 4.1 the setup suffered from problems with the salt bridge connection between the sample channel and the reference cell. This caused the potentiostat to a more negative potential than

the intended -1200 mV_{SCE}. The low potential caused increased hydrogen evolution on the sample plates and increased hypochlorite evolution on the platinum counter electrode. It is very likely that the combination of heat and high concentrations of hypochlorite was highly aggressive towards the coating products, this would explain the severe damage observed, far from the holiday, on most samples in the 18 day test (examples shown in appendix D). This vulnerability to hypochlorite would probably make it prudent to intermittently change the electrolyte in the apparatus to avoid a build-up of hypochlorite, though the evolution of hypochlorite should be limited during normal test conditions. Lower potentials are also known to increase the rate of cathodic disbonding, which would explain the relatively poor performance in the 18 day test compared to the 28 day test.

5.1.2 Time-Dependency of Cathodic Disbonding

As was noted in section 2.2.3, the disbonded area normally propagates linearly with time. From figure 4.2 it was quite clear that this was not the case, when all the results from the HTCD tests were considered. However, the 18 day test was non-standard. Periods of very high current rates, and extensive damage on the samples (section 4.1) may have resulted in quicker than normal cathodic disbonding. Problems with the salt bridge to the reference cell could have caused the potentiostat to polarize the samples to a potential more negative than the intended -1200 mV_{SCE}. A more negative potential would result in a quicker propagation of the cathodic disbonding. This would make the results from the 18 day test incommensurable with those obtained in the 7 and 28 day tests, where the potential was the intended -1200 mV_{SCE}. Therefore, a discussion of the time-dependency of the disbonding should be based on the results from the 7 and 28 day tests, ignoring the 18 day test.

It is important to note that the information that can be gained from a model based on two points (7 and 28 days) is extremely limited. As such it is unfortunate that the 18 day test must be disregarded in this case. Further tests will be required to validate the linear model that is suggested. A linear model is however in accordance with current theory and has been confirmed by numerous studies at ambient temperatures.[1][2][26] A loose estimate of the initiation period can be calculated from these results, provided that the linear model is valid for elevated temperatures.

When the results from the 7 and 28 day tests are considered, only four of the products can be investigated (H, I, K, N). Product R was not included in the 7 day test. Product B gave no disbonding in the 7 day test, which indicates that the initiation period for product B is longer than 7 days (168 hours). Linear regression was used to find the initiation period and rate of propagation for the remaining products. This was displayed for products H, K and N in figure 4.3.

From the resulting linear relations one can see that product H has a very long initiation period(~159 hours), but also a quick propagation rate. This could be seen in the performance of product H, which was excellent in the 7 day test, but mediocre in the 28 day test. A long initation period also explains why product H performed well in previous tests at 160 °C and 180 °C, when the duration of these, 7 days, was only a slightly longer than the initiation period. The extreme thickness of product

H would contribute to the long initation period, which is caused by diffusion and hence dependent on distance. Products K and N have much lower initiation periods (~29 and ~55 hours respectively) and slower propagation rates.

5.1.3 Protection Current in the Accelerated Test

The correlations between the necessary protection current and the performance of various samples in the accelerated tests were very inconsistent. Samples K1 and K3 displayed increased protection currents towards the end of the test, these samples were also quite severely degraded. Samples I3 and R1 also displayed increased protection currents, but these samples were among the least degraded in the test. Samples H1, H3, and K2 had the lowest protection currents of all the samples towards the end of the test, all of these displayed significant disbonding and blistering. Samples I1 and R2 also displayed quite low protection currents, these samples displayed little degradation. The required protection current did not give any indication of the extent of the disbonding on a sample.

The lack of a correlation between the required protection current and the extent of disbonding is in direct conflict with the definition of the Coating Breakdown Factor as presented in the NORSOK standard.[24] The same lack of correlation has been observed previously, with a larger selection of coating products in accelerated tests[3] and in a five year test performed in field conditions.[25] The protection current does not give an indication to the extent of disbonding.

Even though cathodic disbonding does not increase the required protection current by itself, and as such does not qualify as coating breakdown as defined by NORSOK M-503, it is an insidious failure mechanism. Areas suffering from cathodic disbonding are significantly less robust than intact areas. Disbonded areas are easily removed by mechanical means, which would expose large areas of unprotected steel to the environment. This would be of great concern in the field, but factors that would cause disbonded areas to detach are not generally included in laboratory tests. Hence, it is important to test for cathodic disbondment directly as the dangers posed by widespread disbonding is not revealed by electrochemical tests alone.

5.1.4 Comparison of the long term test and the accelerated tests

The 400 day test provides conditions that are much closer to actual field conditions than the accelerated tests. A cathodic protection potential of -1100 mV_{SCE} corresponds to that which aluminium anodes would provide. Seawater was used instead of 3.5 % NaCl and a continuous supply of fresh seawater prevented the build-up of reaction products in the electrolyte. Pressurization by air in the accelerated tests provided an artificially high oxygen concentration in the electrolyte, this was avoided in the 400 day test. With this in mind it can be concluded that the 400 day test should be able to predict field performance with reasonable accuracy.

The oil temperature in the 400 day test was 120 °C, while the accelerated tests

used an oil temperature of 150 °C. Temperatures up to 120 °C are quite common in available oil and gas fields, while higher temperatures occur only in selected fields. The temperature in the accelerated test is therefore close to the temperatures that would be encountered in the most extreme field conditions.

Compared to earlier tests the products that were included in the 7, 18 and 28 day tests were all good candidates. With the exception of product B they all performed very well in the 400 day test, suffering from significantly less disbonding than product C. This makes it hard to compare the results from the 400 day tests to those of the other tests, simply because there is so little spread in the results. For the three products H, I and K there is no direct correlation between the results in the long term test and the accelerated tests. All three coating products performed comparably in the long term test, while there was significant variation in performance in the accelerated tests. Product B disbonded completely in the 400 day test, while it showed moderate disbonding in the accelerated tests.

The accelerated tests are poor indicators of performance in a long term test for product B. Too little information is available to conclusively determine whether the same is the case for the other products. Earlier studies, using the same equipment, showed that the relative performance of the different coatings in accelerated tests was comparable to their relative performance in near field conditions.[38] The temperature difference between the long term test (120 °C) and the accelerated tests (150 °C) probably contributes significantly to the differences. Coating products that undergo specific, temperature dependent changes between 120 °C and 150 °C, such as glass transition, will likely display very different performance at the two temperatures.

5.1.5 Performance Ranking of the Coating Products

The results from the different tests makes it possible to rank the different coatings with regards to high temperature, underwater exposure. This ranking is based partially on the results from the accelerated tests, and partially by the results from the long term tests.

Products I and R are excellent candidates for high temperature underwater exposure. Product R outperformed product I in the only two tests R was included in, but the width of excellent results for product I in this and earlier studies[3][33] gives strong indication of product I's validity. Product R is also quite probably an excellent coating; further testing will be required to confirm this.

Products K and N are both good candidates for high temperature underwater exposure. The two products have performed comparably in most tests they have been included in, though product N performed slightly better at 140 °C.

Product H has performed excellently in all 7 day tests, but suffered from significant disbonding and blistering in the tests with longer duration.

Product B has performed moderately well in the accelerated tests. However, the

complete failure in the long term test is a cause for concern.

All of the included coatings were chosen due to their excellent results in previous tests[3], with the exception of product R. These coatings only appear to perform poorly when compared to other highly advanced coatings. The conditions of the accelerated tests were quite harsh and inadequate coating products would likely fail completely.

With this in mind the included coating products can be ranked by suitability for use on high temperature underwater structures, the first product being the most suitable: Product I, Product R, Product N, Product K, Product H, Product B.

5.1.6 Evaluation of the Apparatus

The HTCD apparatus has been used to produce interesting results in several experiments. The results seem relatively consistent, in accordance with theory and near-field condition tests. The apparatus itself has suffered from several practical problems which will not be discussed in close detail, most of these problems are related to the fact that the apparatus is a prototype that was not originally designed to be pressurized. A lengthy discussion of possible improvements is included in appendix G.

5.2 Oxygen Diffusion

The oxygen diffusion experiment did not yield the information necessary to calculate the diffusion coefficient of oxygen in any of the coating systems tested. A clear change in the measured current is necessary in order to assess the break-through time. In figure 4.6b there was no such change.

The first part of the experiment involved the removal of oxygen from the electrolyte and eventually from the coatings. During this stage the protection current was measured with the reasoning that it would approach zero as the oxygen was depleted. Knudsen found that the current approached 0 pA after 30 days.[2] In this experiment, as is evident from figure 4.6a, samples of product H, I and N started out at near zero protection current. As time went by the protection current actually increased for product H, this was also the case for products B and K, which started at larger values. These results were not in correspondance with those of Knudsen.

In the second part of the experiment the electrolyte was areated abruptly, quickly restoring the oxygen content of the electrolyte. This should have resulted in a break in the protection current from near zero, rising to an equilibrium value. No such break was observed. This behaviour has been observed previously.[2]

Quite thick coating systems were tested and it is possible that oxygen diffusion through these coatings is so slow that this method is unsuitable. The tested coatings were between 600 µm and 1200 µm, the tests performed by Knudsen were on systems with a dry film thickness of 300 µm.[2]

5.3 Electrochemical Impedance Spectroscopy

The electrochemical impedance spectroscopy experiments provided data that is not readily available. That is, impedance data on commercial coating products at temperatures over 100 °C. The general lack of interest in commercial coating systems for scientific studies (model systems are used instead) combined with the difficulties assosciated with performing these experiments at temperatures above the boiling point of the electrolyte makes results of this kind rare.

Impedance was drastically reduced by an increase in temperature, as could be seen in figure 4.7a. This reduction in impedance upon heating was also seen in previous experiments, though that did not include temperatures over 90 °C.[3] Since this change can be observed at low frequencies it can be assumed that the change came about in the processes modelled as resistances in the equivalent circuit diagram, figure 2.3. As noted in section 2.4.2, the measurements were probably dominated by the resistance against ion transport. This was confirmed by linear polarization curves that were recorded in order to verify this. When heating resulted in a drastic reduction in impedance it can therefore be assumed that the resistance against ion transport was weakened.

The reduction in impedance could be observed for all the tested coating products. The magnitude of the impedance, and the magnitude of the change in impedance varied for the different coatings. Products I and N showed clearly higher impedance values than products H and K at temperatures up to 90 °C. Only products I and N were tested above 90 °C. Product I showed a continued decrease in impedance upon heating before it stabilized at around 140 °C. Product N stabilized much sooner, at about 100 °C. This indicates that there is a minimum value for the impedance of a coated system, but this value is, in absolute terms, quite low. The exact level of this minimum value also varies from one coating product to the other.

The experiments performed on coatings that had been previously heated gave interesting results. There was a clear difference in impedance for a coating tested at 30 °C for the first time, and a coating tested at 30 °C after having been previously tested at 90 °C. All the tested products are designed for use at high temperatures, but it seems clear that exposure to these temperatures will cause a lasting decrease in their protective strength. Tests involving long term storage after the heat exposure, before the second low temperature testing, would reveal whether this decrease in impedance is permanent. The relatively small difference between impedance at 30 °C and 50 °C after high temperature exposure suggests that the coatings, after heat exposure, are weakened to a specific level. This specific level is higher than the impedance measured at 90 °C. This was very clear for low frequencies in figure 4.8b. The decreased resistance to ion transport caused by heat exposure can partially be explained by a general increase in diffusion speeds at elevated temperatures. But the difference between previously heated and virgin samples suggest that heat exposure results in lasting change in the coating systems.

5.4 Scanning Electron Microscope

It is interesting to note that the disbonding is so clearly distinguishable in the SEM. The disbonded distance as determined by the SEM method is in close accordance with that measured in the usual manner. Investigation by the SEM is also destructive and is more timeconsuming than the usual method, SEM is therefore not a replacement for the usual method of investigation. However, the great magnification possible in SEM allows close study of details.

The most interesting application of SEM equipment in this field might be the use of EDS to investigate the composition of different species present at or near the interface. The results from the studied sample indicated that calcium and zinc oxides were present in and near the holiday. Calcium oxide has a very low solubility and the precipitation of calcium oxide on the cathode in cathodic protection systems is a well-known phenomena, the calcium ions were present in the electrolyte before being precipitated as oxides. There are two likely sources for the calcium ions. Calcium ions may have been present as an impurity in the NaCl used in the electrolyte. Calcium ions may also have been present in the water used in the electrolyte. Zinc ions were abundant in the electrolyte due to the sacrificial anodes protecting the channel. The existence of calcium and zinc oxides beneath the coating near the holiday suggests the transport of calcium and zinc ions might participate in the general transport of cations along the coating-substrate interface, though the contribution of these low-mobility ions to the speed of cathodic disbonding is probably negligible.

The iron oxide that was identified at the coating-substrate interface might be ferrous oxide. The presence of ferrous oxide would explain the black ring often discovered on the substrate after removal of disbonded coating. No separate iron oxide phase was discernible along the interface far removed from the holiday, suggesting that large deposits of the oxide are indeed the results of disbonding-related reactions.

5.5 Factors Relevant for Cathodic Disbonding Tests

There does not seem to be a clear correlation between performance and generic type. Product B and H are glass-flake epoxies, they are discussed more in depth in the next paragraph. Product I is the only coating of the Bisphenol F type. Bisphenol F is an unusual epoxy resin for subsea coatings, though not unheard of. Bisphenol F resins have been known to possess good heat resistance. Without other products of the same generic type it is impossible to say whether Bisphenol F type coatings in general are well suited for high temperature underwater applications, or if product I is an exceptional coating product. Products K and N are epoxy novolacs, while product R is an epoxy amine type coating. Without further investigation with more coating products of each generic type it is impossible to determine if some generic tpyes are inherently better suited for high temperature underwater applications. Products of several different generic types all performed well in the HTCD tests.

Only two of the tested products were pigmented with glass flakes. Product B, which

was completely disbonded in the 400 day test, but showed an unusual disbonding behaviour as the area closest to the holiday still showed some adhesion while the rest of the exposed area was disbonded. Chemical breakdown of the binder, glass flakes or both caused by the high pH in the disbonded area was suggested as an explanation. Product H was also pigmented with glass flakes, product H suffered from blistering on the 28 day test. Glass flakes are included in coating systems to increas barrier properties. Glass flakes are impermeable to oxygen, water and hydrated ions, they therefore increase the diffusion paths of these species because the species will have to move around the glass flakes. Flake shaped pigments tend to be arranged parallell to the substrate, maximizing their barrier effect. However, if a glass flake is arranged perpendicular to the substrate it may aid in the formation of a conductive pathway. Since glass flakes can be in the same size range as the thickness of the coating system, a single perpendicular glass flake can form a conductive pathway through the entire coating system. As was noted in section 2.2.3 glass flakes have been shown to reduce cathodic disbonding, though not to the same extent as aluminium flakes. None of the experiments in this study indicate that glass flake pigmentation is superior to other pigments.

The cathodic disbonding mechanism requires oxygen transport through the coating. Although oxygen diffusion does not appear to be the rate determining factor it is nevertheless important as cathodic disbonding is halted when no oxygen is available. The oxygen diffusion rate was too low to be accurately measured by the chosen method. Although probably not the most important factor, a low oxygen diffusion rate is nevertheless one of several important factors for an excellent coating system.

There was a correlation between performance in the HTCD tests and results from the EIS experiment. Products I and N, displayed a higher resistivity than the other investigated products. Products I and N also performed very well in the HTCD tests. Product H displayed the lowest resistivity, it was also the only product suffering from extensive blistering in the accelerated tests. Resistivity, in this case, is mostly based on a resistance against ion transport. A low resistance against ion transport may allow ions to migrate through the coating. An accumulation of ions beneath a coating will lead to the an osmotic pressure build-up, and initate blistering.

Investigation using a scanning electron microscope resulted in images where the cathodically disbonded area was visibly distinct from the intact area. More importantly, the occurence of oxides beneath the disbonded coating is a strong indicator that electrochemical reactions occur beneath the coating to some extent, even without a corresponding increase in protection current.

6 Conclusion and Further Work

The HTCD test has continued to give results in accordance with previous experience. The test therefore remains a good candidate for a pre-qualification test for high temperature underwater exposure, despite its complexity, due to the useful data it provides. The apparatus should be improved according to the suggestions given in appendix G before the method is employed as a standard test. Further 28 day tests with identical samples should be performed to ensure that the equipment is not biased with regards to which position along the channels a sample is placed in.

Expansion of the experiments from 7 day tests to 28 day tests allowed a greater differentiation of the candidate coating products. Some coating products that performed well in 7 day tests performed less well in 28 day tests; 28 days is a typical duration for related industry tests. It was difficult to draw conclusions based on the 400 day test, as most of the coatings showed very little cathodic disbonding.

Some products have performed well in all tests they have been included in. Hence, adequate coating products for applications in high temperature steel structures under water are available.

Due to the limited data available it is difficult to ascertain the time dependency of high temperature cathodic disbonding. It is assumed that the dependency is the same as for cathodic disbonding at ambient temperature, i.e. a linear relationship between time and the disbonded area. Further tests of different durations will be necessary to verify the assumption.

The required protection current does not correlate with the extent of the cathodic disbonding of a sample. Measurements of the protection current cannot predict the degradation of coating products in the conditions of this test.

The diffusion coefficient for oxygen in the coatings could not be determined by the selected method. The method used may not be practical for thick coating products. Experiments, using other methdos, should be performed on thick coating systems to determine a reliable test method.

Investigation by electrochemical impedance spectroscopy revealed that the ionic resistance of a coating system is significantly decreased upon heating to the temperatures encountered in the HTCD experiments. A reduction in impedance of several decades was observed for all investigated coating products. A high impedance measured in this experiment correlated with good performance in the HTCD tests. The only product that suffered blistering in the accelerated tests had low impedance values. EIS-studies performed in situ on samples in the HTCD apparatus should be compared to EIS-studies done performed in gradient-free setups to evaluate the effect the thermal gradient has on the ionic resistance of a coating.

Coatings that had previously been heated to high temperatures suffered from a lasting reduction in impedance values, this suggests that the coating products undergo permanent change as a consequence of high temperature exposure.

The extent of cathodic disbonding can be studied without lifting off the coating by studying a cross section with a scanning electron microscope. Oxide inclusions at and near the holiday were found to be mainly zinc and calcium oxides, oxide deposits far removed from the holidat were found to be iron oxides.

References

[1] P. A. Sorensen, S. Kiil, K. Dam-Johansen, C. E. Weinell, Anticorrosive coatings: a review, Journal of Coatings Technology and Research 6, p135-176 (Jun, 2009).

[2] O. Ø. Knudsen, Cathodic disbonding of organic coatings on submerged steel, The Norwegian University of Science and Technology, Department of Machine Design and Materials Technology (1998)

[3] H. Gundersen, High Temperature Cathodic Disbonding of Organic Coatings on Submerged Steel Structures, Specialization Project TMT 4500, The Norwegian University of Science and Technology, Department of Materials Science and Engineering (2010)

[4] Z. Ahmad, Principles of Corrosion Engineering and Corrosion Control, Elsevier (2006)

[5] Norsok M501, Surface preparation and protective coating, Rev 5 (2004)

[6] ISO-12944, Paints and Varnishes—Corrosion protection of steel structures by protective paint systems

[7] P. Carbonini et al., Electrochemical characterization of multilayer organic coatings, Progress in Organic Coatings, 29, p13-20 (1996)

[8] G. Grundmeier, W. Schmidt, M. Stratmann, Corrosion protection by organic coatings: electrochemical mechanism and novel methods of investigation, Electrochimica Acta 45, p2515-2533 (2000)

[9] D. Greenfield, D. Scantlebury, The Protective Action of Organic Coatings on Steel: A Review, The Journal of Corrosion Science and Engineering 3, 5 (2000)

[10] P. A. Schweitzer, Corrosion of linings and coatings: cathodic inhibitor protection and corrosion monitoring, CRC Press (2007)

[11] M. Madhavian, M. M. Attar, Investigation on zinc phosphate effectiveness at different pigment volume concentrations via electrochemical impedance spectroscopy, Electrochimica Acta 50, p4645-4648 (2005)

[12] R. Naderi, M. M. Attar, Cathodic disbondment of epoxy coating with zinc aluminum polyphosphate as a modified zinc phosphate anticorrosion pigment, Progress in Organic Coatings 69, p392-395 (2010)

[13] M. Stratmann, R. Feser, A. Leng, Corrosion Protection by Organic Films, Electrochimica Acta, 39, 8/9, p1207-1214

[14] N. L. Thomas, The barrier properties of paint coatings, Progress in Organic Coatings, 19, p101-121 (1991)

[15] M. W. Kendig, H. Leidheiser Jr., The Electrical Properties of Protective Polymer Coatings as Related to Corrosion of the Substrate, Protective Polymer Coatings, 123, 7, p982-989

[16] U. M. Steinsmo, The Cathodic Properties of Painted Steel, The Norwegian University of Science and Technology (1987)

[17] T. Nguyen, J. B. Hubbard, J. M. Pommersheim, Unified Model for the Degradation of Organic Coatings on Steel in a Neutral Electrolyte, Journal of Coatings Technology, 68, 855, p45-56 (1996)

[18] H. A. Daynes, The Process of Diffusion through a Rubber Membrane, Proceedings of the Royal Society of London, vol 97, no 685, p286-307 (1920)

[19] W. Funke, The role of adhesion in corrosion protection by organic coatings, The Journal of the Oil and Colour Chemists' Assosciation, 68, p229-232 (1985)

[20] J. Marsh, J. D. Scantlebury, S. B. Lyon, The effect of surface/primer treatments on the performance of alkyd coated steel, Corrosion Science, 43, p829-852 (2001)

[21] M. K. Harun, J. Marsh, S. B. Lyon, The effect of surface modification on the cathodic disbondment rate of epoxy and alkyd coatings, Progress in Organic Coatings, 54, p317-321 (2005)

[22] S. Paul, Surface Coatings Science & Technology, Second Edition, John Wiley & Sons (1996)

[23] P. A. Sørensen, S. Kiil, K. Dam-Johansen, C. E. Weinell, Influence of surface topography on cathodic delamination of anticorrosive coatings, Progress in Organic Coatings, 64, p142-149 (2009)

[24] Norsok M-503, Cathodic Protection, Edition 3 (2007)

[25] O. Ø. Knudsen, U. Steinsmo, Current Demand for Cathodic Protection of Coated Steel – 5 years data, Corrosion 2001, paper 01512 (Houston, TX: NACE 2001)

[26] H. Leidheiser Jr., W. Wang, L. Igetoft, The Mechanism for the Cathodic Delamniation of Organic Coatings from a Metal Surface, Progress in Organic Coatings, 11, p19-40 (1983)

[27] P. A. Sørensen, C. E. Weinell, K. Dam-Johansen, S. Kiil, Reduction of cathodic delamination rates of anticorrosive coatings using free radical scavengers, Journal of Coatings Technology and Research, 7, 6, p773-786 (2010)

[28] ISO 15711, Paints and varnishes—Determination of resistance to cathodic disbonding of coatings exposed to sea water

[29] ASTM G8, Standard Test Methods For Cathodic Disbonding of Pipeline Coatings

[30] ASTM G42, Standard Test Method for Cathodic Disbonding of Pipeline Coatings Subjected to Elevated Temperatures

[31] ASTM G95, Standard Test Methids for Cathodic Disbondment of Pipeline Coatings (Attached Cell Method)

[32] O. Ø. Knudsen, T. G Eggen, K. K. Brende, Test Method for Studying Cathodic Disbonding at High Temperature, Corrosion 2010, paper 10007 (Houston, TX: NACE 2010)

[33] O. Ø. Knudsen, K. K. Brende, H. Gundersen, Cathodic Disbonding at High Temperature, Corrosion 2011, paper 11023 (Houston, TX: NACE 2011)

[34] O. Ø. Knudsen, H. Gundersen, Cathodic Disbonding of Organic Coatings at High Temperature, (Eurocorr 2011, to be published)

[35] A. Al-Borno, M. Brown, S. Rao, High Temperature Cathodic Disbondment Tests, Corrosion 2010, paper 10008 (Houston, TX: NACE 2010)

[36] B. Melve, D. Ali, Corrosion Coatings for High Temperature Water Immersion Service, Corrosion 2006, paper 06021 (Houston, TX: NACE 2006)

[37] P. K. Shukla, R. Pabalan, L. Yang, On Development of Accelerated Testing Methods for Evaluating Organic Coating Performance above 100 °C, Corrosion 2010, paper 10006 (Houston, TX: NACE 2010)

[38] K. Brende, High temperature cathodic disbonding, Master Thesis, The Norwegian University of Science and Technology, Department of Materials Science and Engineering (2010)

[39] I. Alig et al. Characterization of coating systems by scanning acoustic microscopy: Debonding, blistering and surface topology, Progress in Organic Coatings, 64, p112-119 (2009)

[40] I. Alig et al. Investigation of delamination mechanisms in polymer coatings by scanning acoustic microscopy, Journal of Physics D: Applied Physics, 44 (2011)

[41] A. Leng, H. Streckel, M. Stratmann, The delamination of polymeric coatings from steel. Part 1, Corrosion Science, 41, p547-578 (1999)

[42] A. Leng, H. Streckel, M. Stratmann, The delamination of polymeric coatings from steel. Part 2, Corrosion Science, 41, p579-597 (1999)

[43] A. Leng, H. Streckel, K. Hofmann, M. Stratmann, The delamination of polymeric coatings from steel. Part 3, Corrosion Science, 41, p599-620 (1999)

[44] R. Posner, M. Santa, G. Grundmeier, Wet- and Corrosive De-Adhesion Processes of Water-borne Epoxy Film Coated Steel, Journal of the Electrochemical Society, 158, pC29-C35 (2011)

[45] P. A. Sørensen, K. Dam-Johansen, C. E. Weinel, S. Kiil, Cathodic delamination of seawater-immersed anticorrosive coatings: Mapping of parameters affecting the rate, Progress in Organic Coatings, 68, p283-292 (2010)

[46] U. Steinsmo, J. I. Skar, Factors Influencing the Rate of Cathodic Disbonding of Coatings, Corrosion 50, p934-939 (1994)

[47] O. Ø. Knudsen, J. I. Skar, Cathodic Disbonding og Epoxy Coatings – Effects of Test Parameters, Corrosion 2008, paper 08005 (Houston, TX: NACE 2008)

[48] W. Zhou, S. J. Edmondson, T. E. Jeffers, Effects of Application Temperature, Degree of Cure and Film Thickness on Cathodic Disbondment of Conventional and New Generation FBE Coatings, Corrosion 2006, paper 06049 (Houston, TX: NACE 2006)

[49] B. Melve, D. Ali, Coatings for High Temperature Water Immersion Service, Materials Performance, August, p30-34 (2006)

[50] W. Vonau, W. Oelßner, U. Guth, J. Henze, An all-solid-state reference electrode, Sensors and Actuators B, 144, p368-373 (2010)

[51] Yuan C., Liang C., An X., Electrochemical Performance of High Purity Zinc and Zn-Al-Cd Alloy as Reference Electrodes, Wuhan University Journal of Natural Sciences 15, 1, p64-70 (2010)

[52] E. C. Bucharsky, E. B. Castro, S. G. Real, An Electrochemical Impedance Spectroscopy Analysis of Protective Behaviour of Final Coatings on Naval Steel, The Journal of Corrosion Science and Engineering, 2, 19 (1999)

[53] A. J. Bard, M. Stratmann, Encyclopedia of Electrochemistry, Volume 3 Instrumentation and Electroanalytical Chemistry, Wiley-VCH Verlag GmbH & Co (2003)

[54] F. Scholz, Electroanalytical Methods, Guide to Experiments and Applications, Springer Verlag (2010)

[55] O. Ø. Knudsen, personal communication, May (2011)

Appendices

A Heat Transport Calculations

A one-dimensional, steady state heat transport model was prepared by Brende[33][38]. The parameters used are presented in table A.1. The parameters for the oil are based on data from the manufacturer, as made available by MatWeb. The parameters for water are based on data from the CRC Handbook of Chemistry and Physics. Parameters regarding bulk temperatures, flow rates, thicknesses and areas were based on measurements taken on the equipment and sample plates. The value used for the thermal conductivity of a coating was the average, as measured on a limited number of coatings.[33]

Based on the parameters in table A.1 and the equations given below, the following temperatures were calculated for each product: T_1, the temperature at the oil-steel interface, T_2, the temperature at the steel-coating interface and T_3, the temperature at the coating-electrolyte interface. These results are presented in table A.2.

The heat transfer by conduction is expressed by Fourier's law of heat conduction, equation A.1. Where Q is the transported heat, k is the thermal conductivity, A is the area perpendicular to the heat transfer and $\frac{dT}{dx}$ is the temperature gradient in the direction of feat transfer.

$$Q = kA\frac{dT}{dx} \tag{A.1}$$

The heat transfer by convection is expressed by Newton's law of cooling, equation A.2. Where h is the convection heat transfer coefficient. T_s is the surface temperature and T_∞ is the temperature in the bulk of the fluid.

$$Q = hA(T_s - T_\infty) \tag{A.2}$$

To find the convection heat transfer coefficient (h) the flow of the oil and the electrolyte must be considered. The Reynold's number can be found by equation A.3, where $\bar{v}$ is the average flow velocity, D is the characteristic length, which is the hydraulic diameter for a non-circular tube and ν is the kinematic viscosity.

$$Re = \frac{\bar{v}D}{\nu} \tag{A.3}$$

Similarly the Prandtl number can be found from equation A.4 where α is the thermal diffusivity given by the ratio between the thermal conductivity, density and specific heat capacity, i.e. $\alpha = \frac{k}{\rho c_p}$.

$$Pr = \frac{\nu}{\alpha} \tag{A.4}$$

For $1.5 < \text{Pr} < 500$ and $3000 < \text{Re} < 10^6$ the flow is turbulent and the Nusselt number can be expressed by equation A.5

$$Nu = 0.012(Re^{0.87} - 280)Pr^{0.4} \tag{A.5}$$

The Nusselt number can be expressed as shown in equation A.6. By entering the value of Nu from equation A.5 and solving for h, the convection heat transfer coefficient can be calculated.

$$Nu = \frac{hD}{k} \tag{A.6}$$

Total heat transfer can also be expressed as $Q = \frac{\Delta T}{R_T}$ Where R_T is the thermal resistance and ΔT is the temperature difference. The conservation of energy yields the relationship $Q_{conv,1} = Q_{steel} = Q_{coat} = Q_{conv,2}$. These can be combined to give equation A.7.

$$Q = \frac{T_{bulk,oil} - T_1}{R_{conv,1}} = \frac{T_1 - T_2}{R_{steel}} = \frac{T_2 - T_3}{R_{coat}} = \frac{T_3 - T_{bulk,water}}{R_{conv,2}} \tag{A.7}$$

This gives $Q = \frac{T_{bulk,oil} - T_{bulk,water}}{R_{Total}}$, where R_{Total} is the sum of all the thermal resistances, since they are considered to be in series. This can be expressed by equation A.8. If the values of h are known, this can be used to calculate the interface temperatures T_1, T_2 and T_3.

$$\begin{aligned} R_{Total} &= R_{conv,1} + R_{steel} + R_{coat} + R_{conv,2} \\ &= \frac{1}{h_o A} + \frac{l_{steel}}{k_{steel} A} + \frac{l_{coat}}{k_{coat} A} + \frac{1}{h_w A} \end{aligned} \tag{A.8}$$

The accuracy of this method was tested by placing a thermocouple beneath the coating on a sample plate. This sample plate with a temperature sensor at the steel-coating interface was then subjected to tests in the HTCD apparatus, the recorded temperatures were compared to the calculated values. Following this investigation, the model presented above was deemed adequatly accurate.[33]

Table A.1: Paramters used in the heat transport calculations

Symbol	**Parameter**	**Value**	**Unit**
$T_{Oil,Bulk}$	Bulk temperature of the oil	423	K
$T_{Water,Bulk}$	Bulk temperature of the electrolyte	303	K
l_{steel}	Sample steel thickness	0.004	m
k_{steel}	Thermal conductivity, steel	43	$\mathrm{Wm^{-1}K^{-1}}$
l_{coatB}	Sample coating thickness product B	0.70	10^{-3} m
l_{coatH}	Sample coating thickness product H	1.07	10^{-3} m
l_{coatI}	Sample coating thickness product I	0.68	10^{-3} m
l_{coatK}	Sample coating thickness product K	0.66	10^{-3} m
l_{coatN}	Sample coating thickness product N	1.04	10^{-3} m
l_{coatR}	Sample coating thickness product R	0.57	10^{-3} m
k_{coat}	Thermal conductivity, coating	0.25	$\mathrm{Wm^{-1}K^{-1}}$
l	Length of channel	1.68	m
A	Exposed sample area	0.0048	$\mathrm{m^2}$
$\bar{v}_{el}$	Average electrolyte flow velocity	0.2	$\mathrm{m\ s^{-1}}$
$D_{h,el}$	Hydralic diameter of electrolyte channel	0.047	m
ν_w	Kinematic viscosity, water, 30 °C	$8.01 \cdot 10^{-7}$	$\mathrm{m^2s^{-1}}$
k_w	Thermal conductivity, water, 30 °C	0.6155	$\mathrm{Wm^{-1}K^{-1}}$
Pr_w	Prandtl number, water, 30 °C	5.41	–
Re_w	Reynolds number, water	11740	–
Nu_w	Nusselt number, water	75	–
h_w	Convection heat transfer coefficient, water	986	$\mathrm{Wm^{-2}K^{-1}}$
$\bar{v}_{oil}$	Average oil flow velocity	1.13	$\mathrm{m\ s^{-1}}$
$D_{h,oil}$	Hydraulic diameter of oil channel	0.011	m
$\nu_{o,150}$	Kinematic viscosity, oil, 150 °C	$2.09 \cdot 10^{-6}$	$\mathrm{m^2s^{-1}}$
$k_{o,150}$	Thermal conductivity, oil, 150 °C	0.1259	$\mathrm{Wm^{-1}K^{-1}}$
$Pr_{o,150}$	Prandtl number, oil, 150 °C	30.13	–
$Re_{o,150}$	Reynolds number, oil, 150 °C	5947	–
$Nu_{0,150}$	Nusselt number, oil, 150 °C	77	–
$h_{o,150}$	Convection heat transfer coefficient, oil	880	$\mathrm{Wm^{-2}K^{-1}}$

Table A.2: Results of the heat transport calculations

Product	**Location**	**Temperature [K]**
B	Oil-Steel Interface	396
B	Steel-Coating Interface	394
B	Coating-Electrolyte Interface	327
H	Oil-Steel Interface	402
H	Steel-Coating Interface	400
H	Coating-Electrolyte Interface	322
I	Oil-Steel Interface	395
I	Steel-Coating Interface	393
I	Coating-Electrolyte Interface	328
K	Oil-Steel Interface	395
K	Steel-Coating Interface	393
K	Coating-Electrolyte Interface	328
N	Oil-Steel Interface	402
N	Steel-Coating Interface	400
N	Coating-Electrolyte Interface	322
R	Oil-Steel Interface	393
R	Steel-Coating Interface	390
R	Coating-Electrolyte Interface	330

B Previous HTCD Test Results

Several of the coating products tested in this work were previously tested by Brende, Knudsen and myself.[3][33][34][38] Results from these previous studies are included in table B.1. The results are presented as disbonded radius in mm. Note that some of the oldest results [38] were later re-evaluated[3][34], the latest evaluation is used in table B.1.

Table B.1: Previous HTCD Test Results

Product	**T_{oil} =120 °C**	**T_{oil} =140 °C**	**T_{oil} =160 °C**	**T_{oil} =180 °C**
A	0.76 ± 0.69	0	0	–
B	0	0	X	–
C	3.44 ± 2.0	6.17 ± 1.12	X	–
D	0	1.00	1.50 ± 0.71	–
E	1.00	–	–	–
F	8.08 ± 1.32	8.67 ± 3.33	X	–
H	0	0	0	1.40 ± 0.10
I	0	0	0	0.13 ± 0.18
J	0	–	–	–
K	0	1.12 ± 0.97	2.36 ± 0.26	–
L	0	0	0	1.92 ± 0.73
M	2.48 ± 1.06	2.23 ± 0.26	4.45 ± 0.92	2.21 ± 0.68
N	0	0	2.00	–
O	3.40	4.75	X	–
P	6.72 ± 0.91	X	X	–
Q	–	–	–	1.09 ± 0.98

X — The sample failed through blistering or excessive disbonding
– — The sample was not tested

C An Alternate Method for Assessing the Disbonded Area

Assessing the disbonded area for very thick and hard coatings can be difficult. The scalpell that is normally used to perform the crossing cuts and the subsequent lift or peel breaks easily. More solid knives may perform without undue breakage, but have resulted in more extensive scratching of the surface beneath the coating. An alternate method, where a sturdy knife or sharp chisel is used to chip away the coating in an area around the holiday larger than the extent of the disbonding, is proposed. After the coating has been thus removed a discolored area on the substrate is clearly visible. The exact appearance of the discolored area differs from sample to sample, though a darkened ring is by far the most common. It is almost impossible to discern the strength of adhesion with this method, but the discolored area provides visual proof of the minimum extent of chemical changes beneath the coating. The images included here, figures C.1a, C.1b, C.1c, C.1d, C.1e and C.1f, show sample plates where the usual method of assessment was utilized around three quarters of the circumference of the holiday, while the new method was used along the last quarter. As can be seen, there is close, but not exact, correlation between the discolored area and the area that is easily lifted with a scalpel.

Products I (C.1c), K (C.1d) and N (C.1e) are examples were the discolored area is easily distinguishable. The contrast between the discolored area and the substrate in general is less obvious for products B (C.1a) and H (C.1b), though easily distinguishable in good light.

(a) Product B

(b) Product H

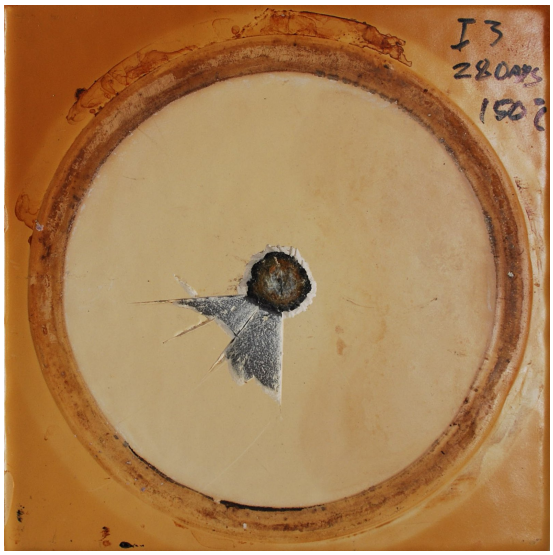

(c) Product I

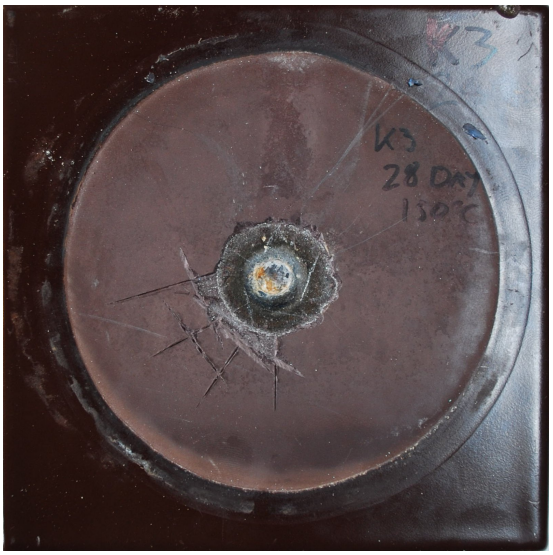

(d) Product K

(e) Product N

(f) Product R

Figure C.1: Samples Dual-Tested with two Methods of Assessment

h

D Images of Tested HTCD Samples

Images taken of different samples studied in the HTCD Apparatus are included below.

In figure D.1 a cracked sample of product K from the 28 day test is shown. This was the only example of a cracked coating encountered during the experiment.

In figure D.1 two sample plates from the 18 day test are shown. Figure D.1c shows a sample of product R where damage along the edge is clearly visible. Figure D.1d shows a sample of product B where the damaged along the edge has been scraped in the fashion usually employed to assess the extent of disbonding, exposing the substrate underneath.

In figure D.2 two blistered samples are shown. Figures D.2a and D.2b show a detail of a sample plate of product N with tiny blisters located near the holiday and an overview picture of the sample after assessment. Figures D.2c and D.2d show a sample plate of product H with severe blistering before (D.2c) and after (D.2d) assessment.

(a) Product K, Cracked

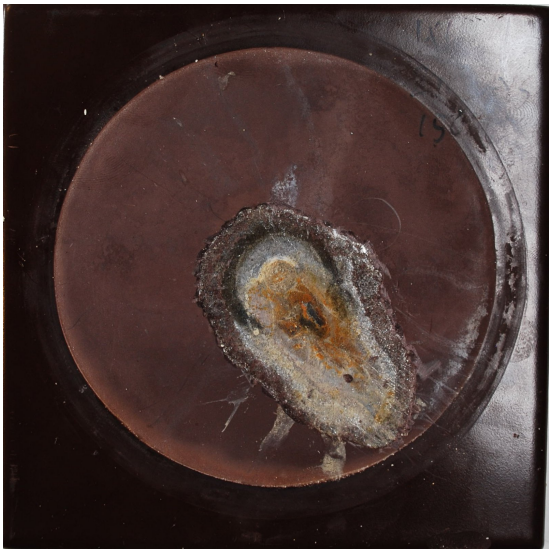

(b) Product K, Cracked, After Asessment

(c) Product R, Showing damage along the edge

(d) Product B, Showing damage along the edge

Figure D.1: Damaged Samples

(a) Product N, blistering in the disbonded area

(b) Product N, after assessment

(c) Product H, extensive blistering

(d) Product H, after assessment

Figure D.2: Products Showing Blistering

E Expanded EIS Results

Electrochemical impedance spectroscopy scans of products H, I, K and N for several temperatures from 30 °C to 150 °C are included in the following figures. Two graphs are provided for each product, one shows the impedance of the coating system, the other the bulk resistivity of the coating product after film thickness and the size of the exposed area has been taken into account.

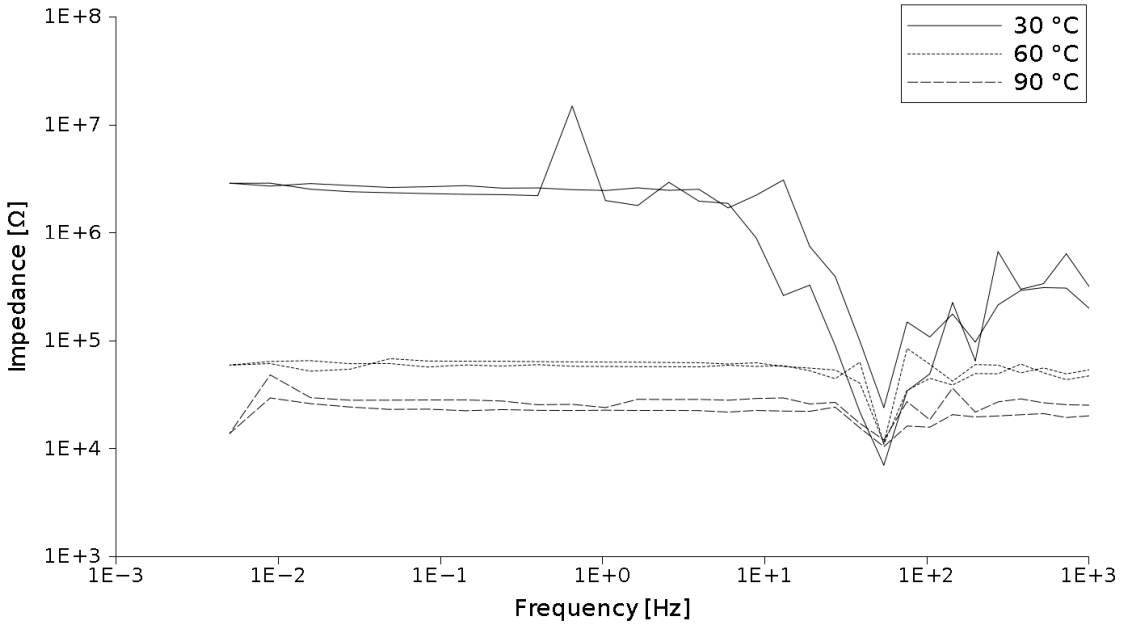

(a)

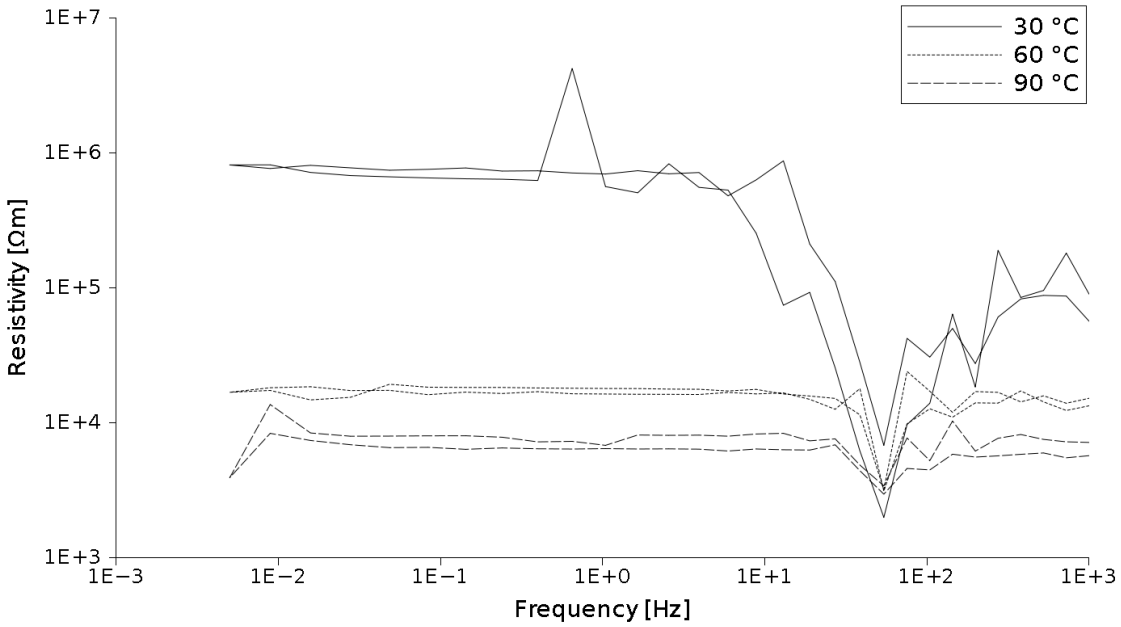

(b)

Figure E.1: EIS Results for Product H

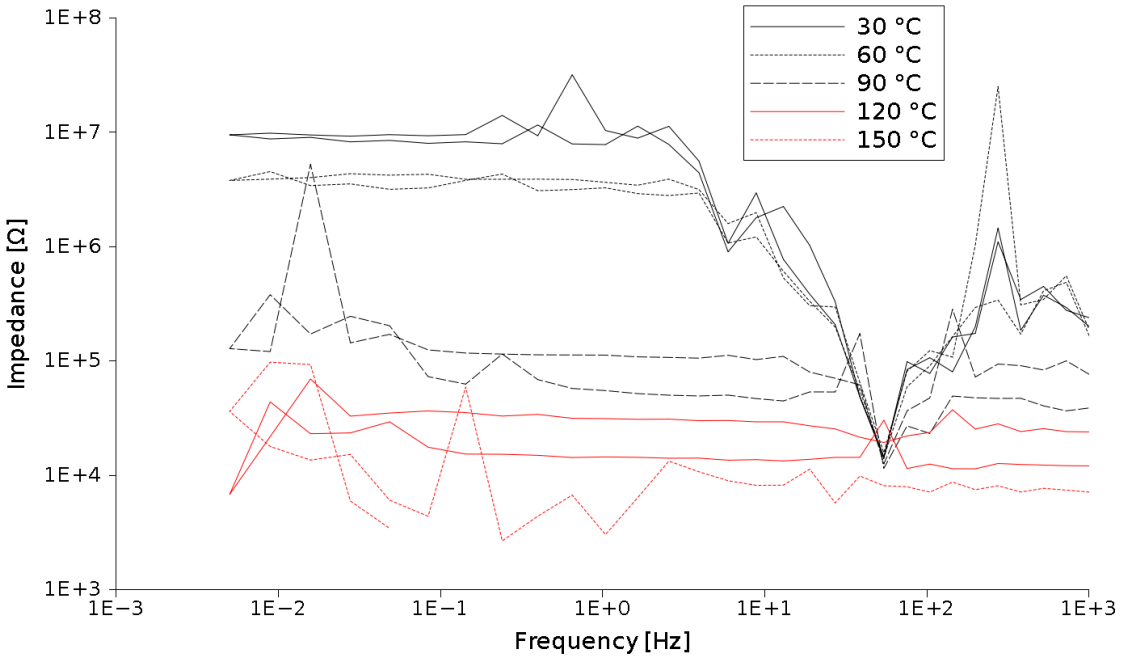

(a)

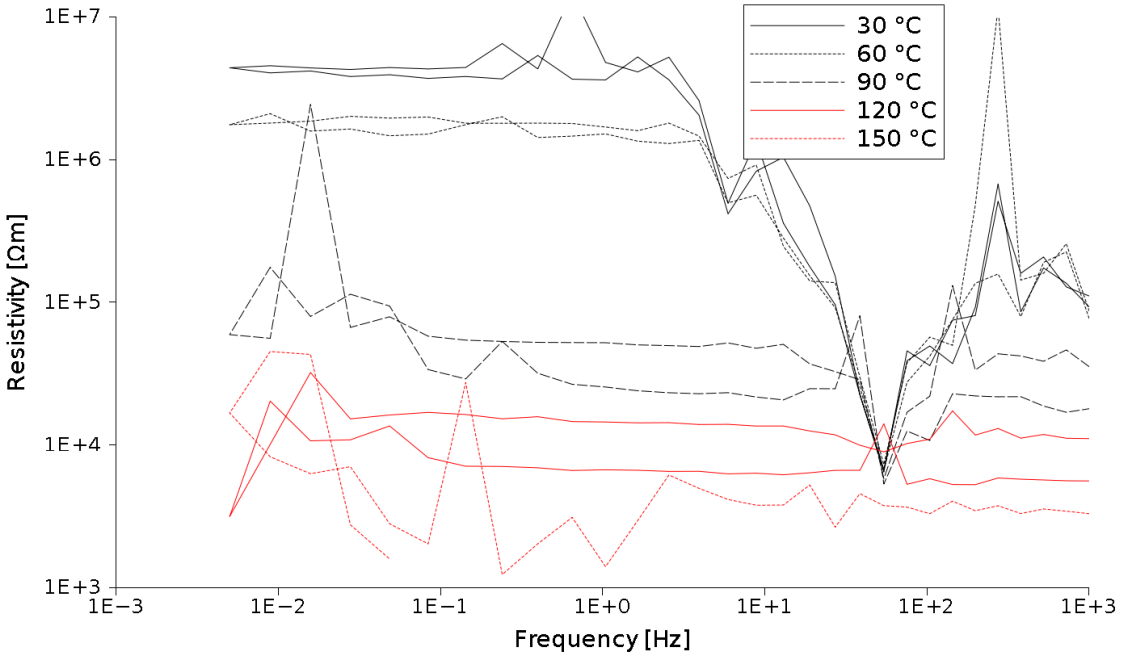

(b)

Figure E.2: EIS Results for Product I

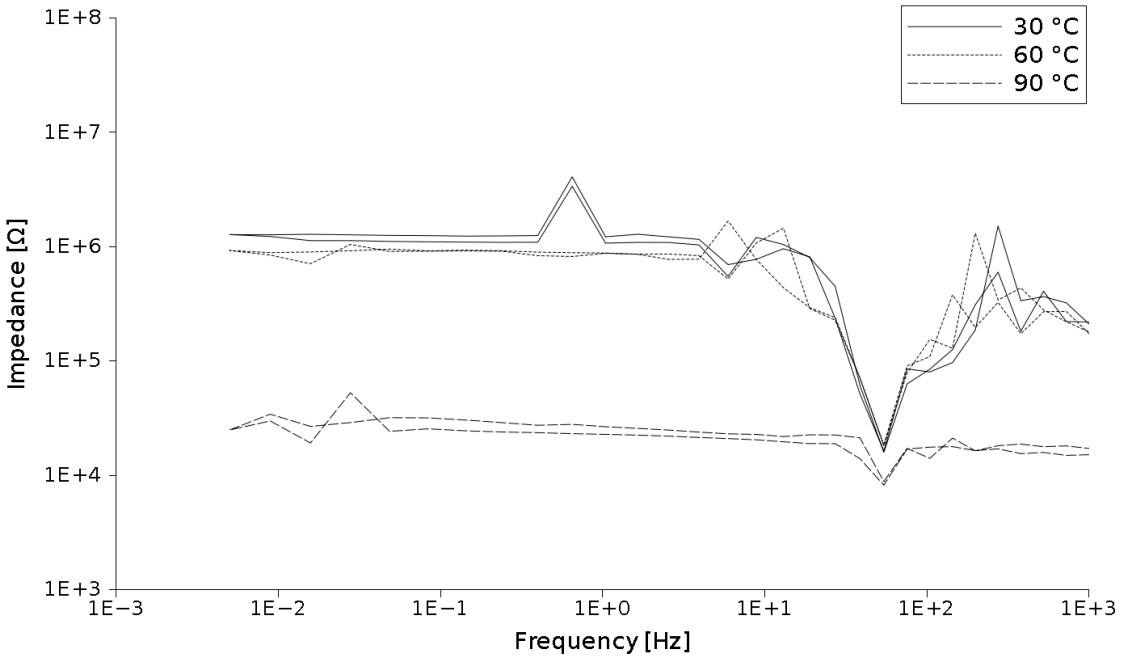

(a)

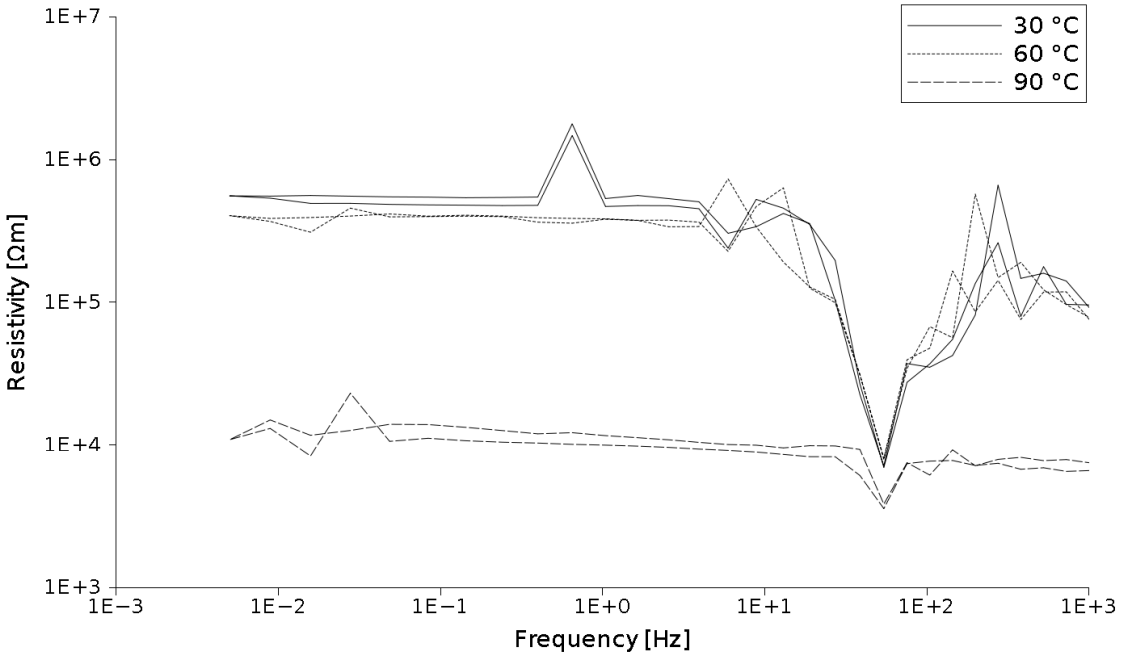

(b)

Figure E.3: EIS Results for Product K

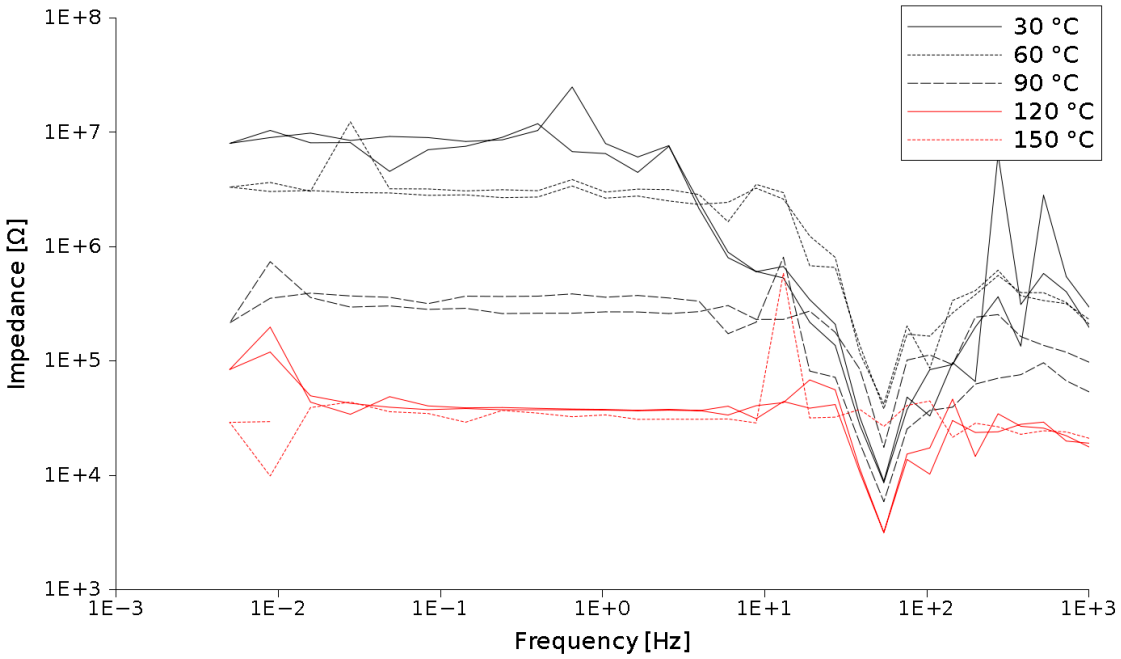

(a)

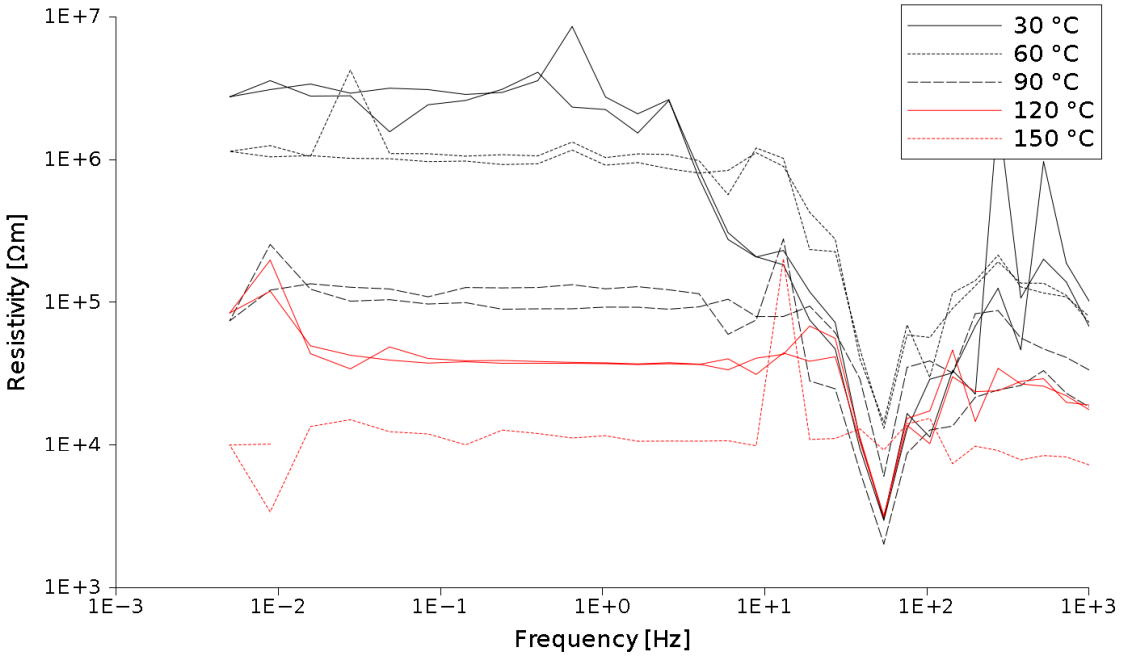

(b)

Figure E.4: EIS Results for Product N

F EDS Spectra

Electron-dispersice X-ray spectroscopy was used to study oxide inclusions observed near the holiday and at the substrate-coating interface. Spectra identified as mainly calcium and zinc oxides (figure F.1a) and iron oxides (figure F.1b) are included.

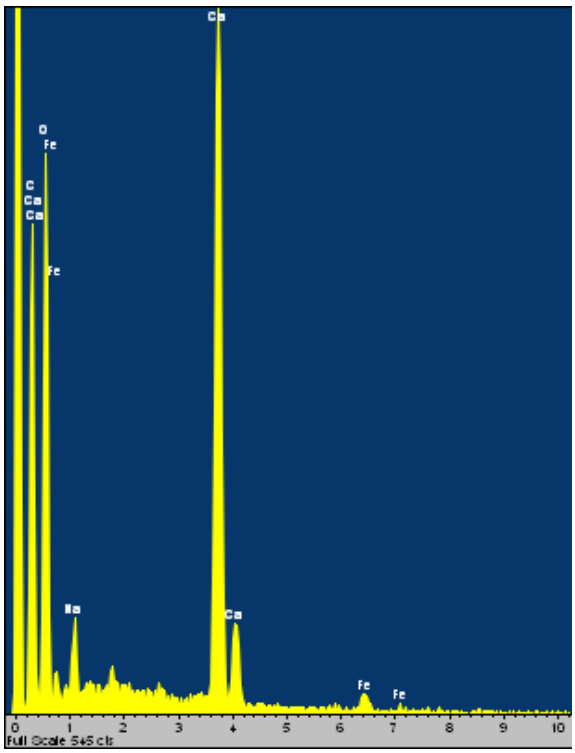

(a) Calcium/Zinc Oxides

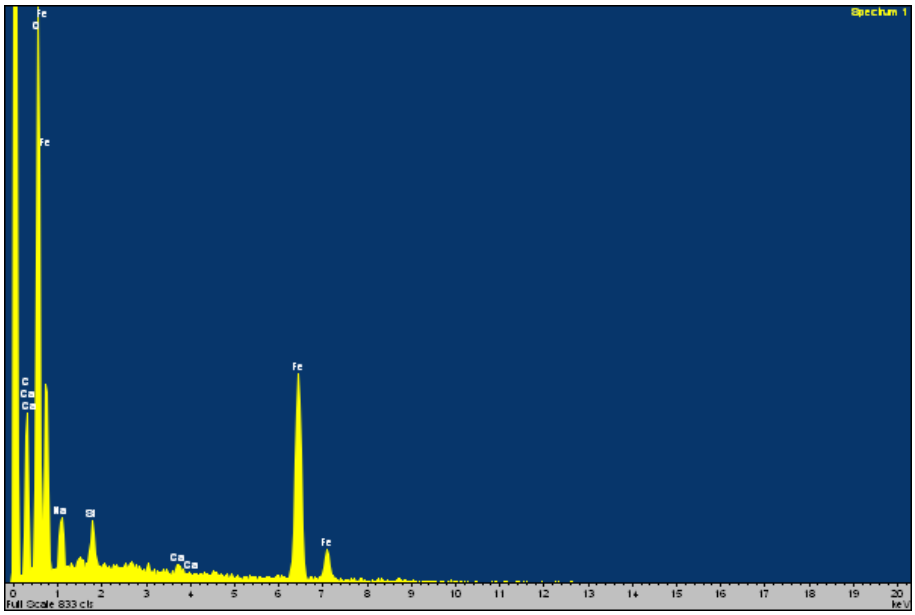

(b) Iron Oxides

Figure F.1: EDS Spectra, from the SEM investigation of oxide inclusions

G Recommendations for Changes to the HTCD Apparatus and Test

Several practical problems were discovered during the work performed with the HTCD apparatus. Several problems are clearly caused by working with a prototype and can easily be corrected, others require a slight redesign of the apparatus or a change in the experimental procedure.

G.1 Leakage

Leakage was a commonly encountered problem. The causes of leakage were legion, but several main culprits could be identified.

Make sure all tubing, nipples and hose clamps are of compatible sizes. When building equipment intended for long-term testing an investment in the correct parts is often preferable to building with whatever is at hand.

The Pt-wire used as a counter electrode for the cathodic protection was originally drawn through two holes in the channel wall which were subsequently filled with silicone glue. This solution proved adequate before the equipment was pressurized. To avoid leakage while the equipment is pressurized the following solution is suggested. The hole should be of a larger diameter and threaded, so as to allow a pipe fitting with male threads to be affixed to the channel. The wire should be drawn through a thin pipe which is then filled with epoxy-glue to provide a gas-proof, heat-resistant seal. The wire-in-pipe connector is then affixed to the pipe fitting.

The ionic connection described by Knudsen and Brende was a cotton thread, soaked in electrolyte, drawn through a plastic tube equipped with clamps to retain the pressure.[38][32] After several incidents involving the ionic connection it was replaced by a different system. The electrolyte channel should be equipped with a threaded hole large enough to accomodate a wooden plug ionic connector of the type used in autoclaves. The wooden plug is soaked in KCl before mounting in the channel to ensure a good ionic connection. The wooden plug provides a pressure-resistant connection, removing the need for clamping.

An alternative for the ionic connection described above is an all-solid zinc reference electrode. An unsuccessfull attempt at using a zinc electrode was made, but a zinc electrode is a viable option according to theory.

The apparatus was fitted with a drainable trough to catch any spillage. It is extremely difficult to avoid all sorts of spillage with this equipment. Some sort of system to catch spillage, or a waterproof floor with a drain, is necessary.

G.2 Ease of Use

Several possible changes that would make the apparatus easier to operate were identified during the course of this work.

The oil channel should be equipped with a valve to allow easy draining of the oil. The oil must be drained every time the samples are changed, the current method of draining involved propping the channel in a slanted position and draining through the oil hose couple.

The X-rings used to complete the seals between the samples were gradually broken down and most had to be replaced after every experiment. The X-rings often stuck to the sample plates after the tests had completed, this resulted in X-rings being ripped loose from the apparatus when the samples were dismounted. Applying grease to the X-rings prior to mounting the samples reduced the extent of this problem.

Leakage resulted in a need to replace the electrolyte in the reservoir. The valve tree on the electrolyte reservoir should allow refilling of lost electrolyte without complete disassembly.

The hoses attached to the electrolyte and oil channels has to be disconnected to dismount the sample plates. These hoses should be connected by quick couplers to make connection and disconnection easier.

A centrifugal pump was used to circulate the electrolyte in the apparatus. The centrifugal pump provided more circulation than what was required, but could not be regulated directly. To compensate for this a dead-loop was installed, the hose leading to the electrolyte channel was fitted with a gate valve to regulate the flow of electrolyte. It was possible, but tricky, to regulate the water flow to the desired flow rate using this system. A displacement pump would make it easier to ensure the correct flow rate, it would also make pump priming easier.

The channel had room for fifteen samples and was relatively difficult to handle. Fifteen samples with two x-rings each means there were thirty potential leaks every time the equipment was assembled. There was no way to remove a single faulty x-ring without disassembling the whole length of the channel. A shorter channel would make it easier to line up all the x-rings correctly before tightening the clamps that fixed the channels together. In the interest of keeping the same capacity, multiple shorter channels in paralell could be used. A shorter channel would also make the equipment easier to move, as the channels constitute the largest, heaviest parts excluding the electrolyte reservoir.

G.3 Corrosion and Durability

The following changes and advice are provided, mainly to ensure a long lifetime of the apparatus and all its parts.

The temperature tolerance of X-rings, as stated by the manufacturers, often differ

between short term and long term exposure. Long term exposure in this case is rarely as long as 28 days. Since the X-rings must be able to withstand the high temperature for 28 days, materials with a stated temperature somewhat higher than the target temperature should be used. Fluroelastomers were succesfully used for oil temperatures up to 160 °C, polytetrafluoroethylene (PTFE) was succesfully used for oil temperatures up to 180 °C.

The electrolyte channel and reservoir were protected by sacrificial zinc anodes in the original design. This resulted in a great deal of zinc oxide in the electrolyte. Before the onset of this work, the electrolyte channel was painted on the inside to reduce anode consumption. The electrolyte reservoir was fitted with a counter electrode and cathodic protection was applied by imposed current. This greatly reduced the anode consumption as well as the amount of zinc oxide in the system. Towards the end of the experiment it became apparent that the electrolyte reservoir had suffered from corrosion despite the cathodic protection. The required protection current for a passive stainless steel reservoir should be relatively low, but care should be taken to ensure that the correct potential is applied by the potentiostat.

G.4 Accuracy

There is no great concern regarding the general accuracy of the equipment. However an experiment proving that the apparatus is unbiased with regards which end of the channel a sample is positioned at has yet to be performed. The following suggestions mainly concern reducing any differences between the two ends, and increasing the general reproducibility and accuracy of the test.

The original design had the oil and the electrolyte flowing in opposite direction, forming a countercurrent heat exchanger. In the interest of providing as similar conditions as possible in both ends of the channels it would be better to have the oil and electrolyte flow in the same direction, forming a parallel heat exchanger. In a paralell flow setup the oil will be warmer in the end where the water is colder, in the other end the oil will be less warm while the water is less cold. The overall effect of a paralell flow setup is a smaller change in the thermal gradient and coating-substrate interface temperature from one end of the channel, to the other.

If shorter channels were implemented, as suggested above, the differences between the two ends of the channel would be reduced. The temperature change from one end of the equipment to the other is relatively minor, but the flow properties of the electrolyte, oil or both may change greatly over the length of the channel.

Salt water (3.5% NaCl (aq)) was used as the electrolyte in the experiment. The electrolyte was based on regular tap water, which resulted in calcium oxide deposits in the holidays on the samples. Preferentially, for a standardized test, either an NaCl solution based on distilled water or artificial seawater based on distilled water should be used.

The protection current was logged throughout the experiment. The protection current is not a good indicator of the extent of disbonding. Drastic changes in

the protection current indicate that something is wrong with the experiment, but deducing what has gone wrong based on current data alone is not nescessarily easy. In addition to the protection current the potential of the sample plates should be measured. The potential is a much better indicator of whether the experiment is going as planned, espescially when combined with current data.